THE GEOLOGICAL SOCIETY OF AMERICA®

Using ignimbrites to quantify structural relief growth and understand deformation processes: Implications for the development of the Western Andean Slope, northernmost Chile

M.E. van Zalinge[1,*], R.S.J. Sparks[1], L.A. Evenstar[1], F.J. Cooper[1], J. Aslin[1], and D.J. Condon[2]
[1]SCHOOL OF EARTH SCIENCES, UNIVERSITY OF BRISTOL, WILLS MEMORIAL BUILDING, QUEENS ROAD, CLIFTON, BRISTOL, BS8 1RJ, UNITED KINGDOM
[2]BRITISH GEOLOGICAL SURVEY, NERC ISOTOPE GEOSCIENCES FACILITIES, NICKER HILL, KEYWORTH, NOTTINGHAM, NG12 5GG, UNITED KINGDOM

ABSTRACT

Large-volume ignimbrites are excellent spatial and temporal markers for local deformation and structural relief growth because they completely inundate and bury the underlying paleotopography and leave planar surfaces with relatively uniform, low-gradient slopes dipping less than 2°. Using one of these planar surfaces as a reference frame, we employed a line-balanced technique to reconstruct the original morphology of an ignimbrite that has undergone postemplacement deformation. This method allowed us to constrain both the amount of posteruptive deformation and the topography of the pre-eruptive paleolandscape. Our test case was the unwelded surface of the 21.9 Ma Cardones ignimbrite, located on the western slope of the Central Andes in northernmost Chile (18°20′S). By reconstructing the original surface slope of this ignimbrite, we demonstrate that the pre–21.9 Ma topography of the Western Andean Slope was characterized by structural relief growth and erosion in the east, and the creation of accommodation space and sedimentation in the west. The paleoslope at that time was dissected by river valleys of up to 450 ± 150 m deep that accumulated great thicknesses (>1000 m) of the Cardones ignimbrite, and likely controlled the location of the present-day Lluta Quebrada as a result of differential welding compaction of the ignimbrite. Our reconstruction suggests that growth of the Western Andean Slope had already started by ca. 23 Ma, consistent with slow and steady models for uplift of the Central Andes. Subsequent deformation in the Miocene generated up to 1725 ± 165 m of structural relief, of which more than 90% can be attributed to fault-related folding of the ~40-km-wide Huaylillas anticline. Uplift related to regional forearc tilting is less than 10% and could have been zero. The main phase of folding likely occurred in the mid- to late Miocene and had ceased by ca. 6 Ma.

LITHOSPHERE; v. 9; no. 1; p. 29–45; GSA Data Repository Item 2016360 | Published online 15 December 2016 doi:10.1130/L593.1

INTRODUCTION

Subduction-related ignimbrite flare-ups, typically lasting for several million years, occurred in the Great Basin, United States, and the Central Andes, South America, during the Cenozoic (e.g., de Silva, 1989; Best et al., 2009). During these flare-ups, large-magnitude eruptions produced ignimbrites with individual volumes of a few hundred to a few thousand cubic kilometers. Ignimbrites can cover areas of thousands of square kilometers, changing the landscape dramatically. The thickness of an ignimbrite is controlled by the total volume erupted, discharge rate, and flow velocity of the pyroclastic flow, as well as the underlying topography. In general, thicker deposits are found in valleys and depressions, while thinner deposits occur on topographic highs (e.g., Walker et al., 1980; Wright et al., 1980; Walker, 1983; Wilson and Hildreth, 1997; Henry and Faulds, 2010; Cas et al., 2011; Roche et al., 2016). The largest ignimbrites can completely inundate and bury the topography, leaving planar regional ignimbrite surfaces with very low slopes (e.g., Walker, 1983). Consequently, these ignimbrite surfaces make excellent spatial and temporal paleomarkers for recording deformation. By applying a line-balanced reconstruction technique to the top surface of an ignimbrite, we demonstrate that it is possible to constrain both the postemplacement deformation of an ignimbrite and the pre-emplacement paleotopography.

In this study, we used the deformed large-volume (>1260 km^3; García et al., 2004) Cardones ignimbrite, dated at 21.9 Ma (van Zalinge et al., 2016), to reconstruct the pre- and posteruptive deformation history of the Western Andean Slope in northernmost Chile. The ignimbrite buried the underlying paleotopography across the Western Andean Slope and is exceptionally well preserved due to the hyperarid climate in the region (e.g., Dunai et al., 2005; Kober et al., 2007; Evenstar et al., 2009). Multiple 1-km-deep drill holes and field outcrops in a 1700-m-deep river valley (the Lluta Quebrada) provide detailed information about the distribution, thickness, and deformation of the Cardones ignimbrite as well as its stratigraphic relationship with older and younger lithologies. The timing of local deformation was determined by dating deformed lithologies as well as younger, overlying, undeformed deposits with U-Pb zircon geochronology. Consequently, in this article, we quantify and constrain the Cenozoic development of structural relief in the study area, which

*E-mail: m.vanzalinge@bristol.ac.uk
Marit van Zalinge http://orcid.org/0000-0002-8349-5648

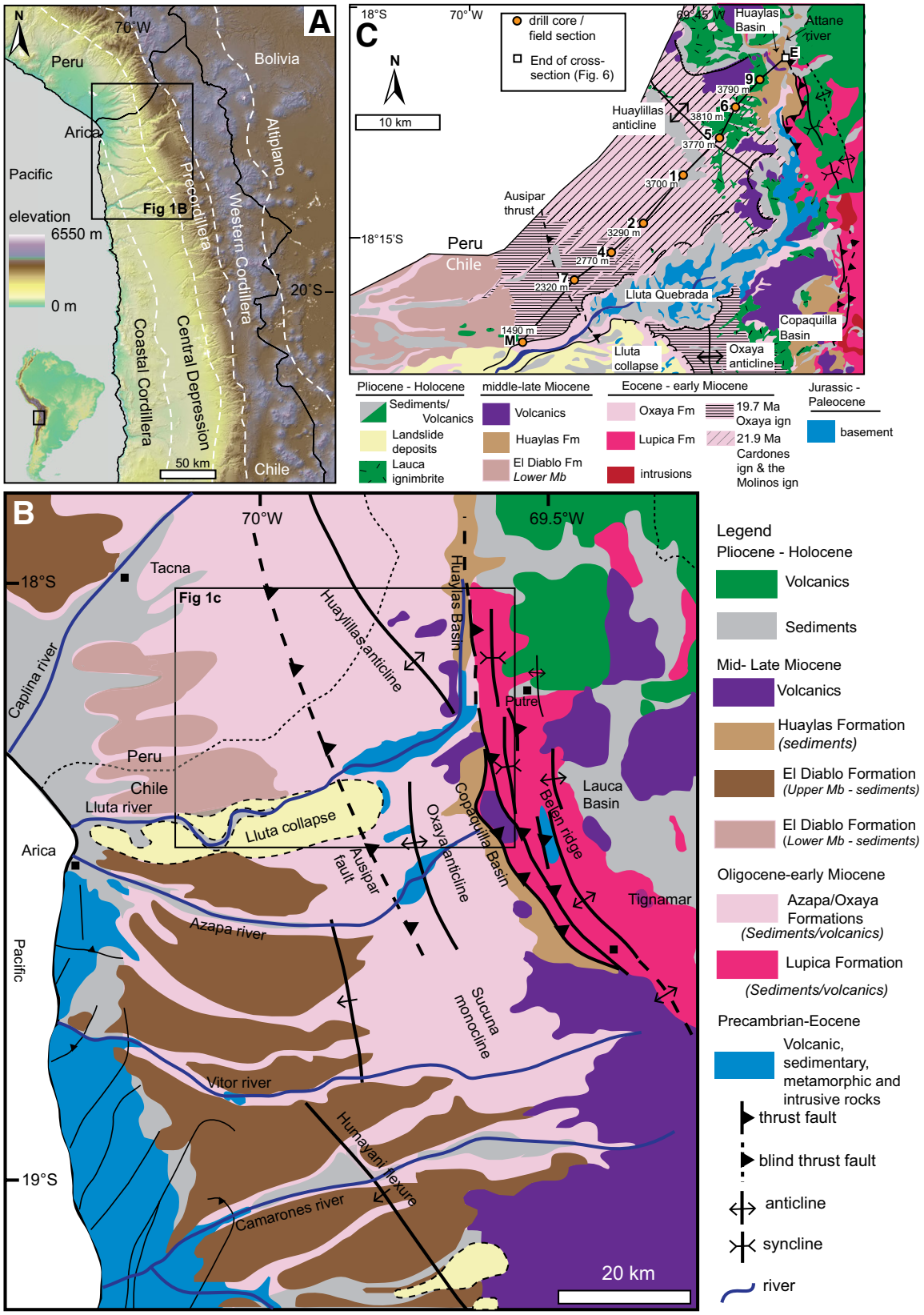

Figure 1. (A) Digital elevation model of the Central Andes in northern Chile indicating the different morphotectonic units from García et al. (2011). (B) Simplified geological map of northern Chile (modified from García et al., 2011). (C) Detailed geological map of the study area modified from García et al. (2004), showing the drill-hole locations and the location of the Molinos section (topographic elevation is indicated next to each location). The geology of Peru is not shown.

indicates that growth of the Western Andean Slope in northern Chile had started by ca. 23 Ma. We subsequently place the results in a wider context and discuss the tectonic controls on timing and amount of deformation as well as landscape evolution.

GEOLOGICAL BACKGROUND

The Central Andes result from ongoing subduction of the Nazca plate beneath the South American plate since Jurassic time (e.g., Coira et al., 1982; Jordán et al., 1983; Isacks, 1988). In northern Chile (18°S–21°S), the present-day western flank of the Central Andes is typically divided into five morphotectonic units. From west to east, these are: the Coastal Cordillera, the Central Depression, the Precordillera, the Western Cordillera, and the Altiplano (Fig. 1A; e.g., Muñoz and Charrier, 1996; García and Hérail, 2005; García et al., 2011; Charrier et al., 2013). In this study, we focus on the Central Depression, Precordillera, and Western Cordillera in northernmost Chile around 18°20′S (Figs. 1B and 1C), which together constitute the Western Andean Slope.

Within the study area, the Coastal Cordillera is absent, and the Central Depression continues across to the Pacific Ocean. Here, the basin is ~45 km wide and reaches a maximum elevation of ~2000 m on its eastern side, where it borders the Precordillera. The Central Depression and Precordillera are separated by the blind west-vergent Ausipar thrust (e.g., Muñoz and Charrier, 1996; García et al., 2004; García and Hérail, 2005; Charrier et al., 2013). The Precordillera is ~30 km wide and increases in elevation from ~2000 m to ~4000 m from west to east. This morphotectonic unit is characterized by two N-S–trending long-wavelength fold structures known as the Huaylillas anticline and the Oxaya anticline, which lie north and south of the Lluta Quebrada, respectively (Fig. 1B). South of the Azapa Quebrada, the Oxaya anticline merges with the Sucuna monocline. Two <10-km-wide, elongate basins are located on the eastern limbs of the two anticlines: the Huaylas Basin to the north and the Copaquilla Basin to the south (e.g., García et al., 2004). A narrow fold-and-thrust belt bounds the Copaquilla Basin and the southern part of the Huaylas Basin to the east, marking the start of the Western Cordillera and the end of the Precordillera (e.g., Muñoz and Charrier, 1996; García et al., 2004; García and Hérail, 2005). East of the Oxaya anticline, this fold-and-thrust belt gives rise to the 4500–5000-m-high Belen Ridge, which is absent to the east of the Huaylillas anticline. The active volcanic arc has been located along the Western Cordillera since the Oligocene (e.g., Coira et al., 1982; Mamani et al., 2010), giving rise to peaks up to 6350 m in elevation (e.g., García and Hérail, 2005).

Stratigraphy and Cenozoic Deformation History

Lithologies in the study area (Fig. 1C) range in age from Jurassic to Pliocene. The simplified stratigraphy is presented in Figure 2. In the Precordillera, basement rocks consist of Jurassic–Cretaceous sediments intruded by the Late Cretaceous–Paleocene Lluta batholith (e.g., García et al., 2004). The basement rocks crop out in places where the Precordillera is deeply incised by rivers (Fig. 1B). During the Eocene–Oligocene, a period of flat-slab subduction with a convergence rate of 60–100 mm/yr (Somoza, 1998) is thought to have triggered incipient uplift of the Western Andean Slope (e.g., Isacks, 1988; Lamb and Hoke, 1997; Wörner et al., 2000; Kay and Coira, 2009; Martinod et al., 2010). During this time, basement rocks were exhumed and uplifted in the Precordillera while contemporaneous accommodation space was created in the Central Depression. Fluvial-alluvial sediments (the Azapa Formation) shed from this emerging paleo-Precordillera and were transported westward to be finally deposited in the Central Depression (Fig. 2; e.g., Wörner et al., 2002; García et al., 2004; García and Hérail, 2005; Wotzlaw et al., 2011).

In the late Oligocene, the subducting slab steepened, and the convergence rate increased to ~150 mm/yr (Somoza, 1998), associated with a major pulse of silicic ignimbrite volcanism in the early Miocene (e.g., Isacks, 1988; Wörner et al., 2000; Hoke and Lamb, 2007; Kay and Coira, 2009). A series of large-volume ignimbrites, known as the Oxaya Formation, was emplaced on the Western Cordillera, Precordillera, and the Central Depression. The caldera complexes associated with these ignimbrites have not been definitively identified, but their sources were likely located to the east of the study area (García et al., 2000). In the Precordillera and the Central

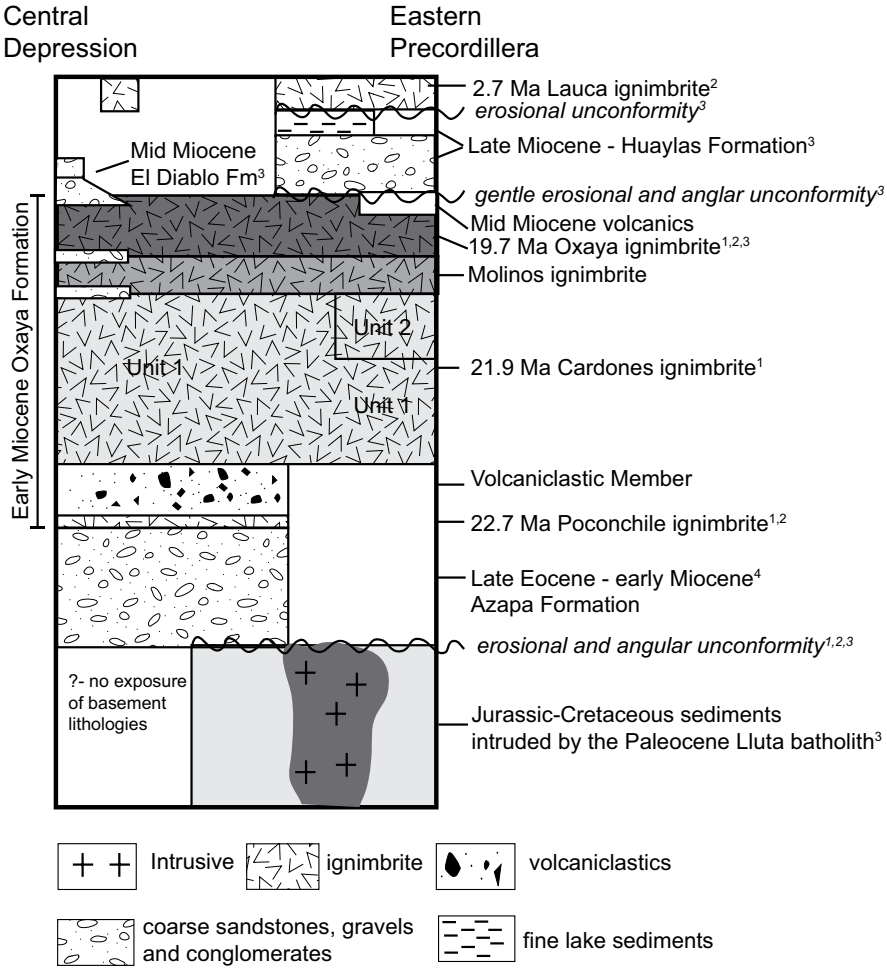

Figure 2. Simplified stratigraphy of the Central Depression and the Precordillera. Data were compiled from: 1—van Zalinge et al. (2016); 2—Wörner et al. (2000a); 3—García et al. (2004); 4—Wotzlaw et al. (2011).

Depression, the Oxaya Formation was deposited between 22.7 and 19.7 Ma and consists of five members, from oldest to youngest: the Poconchile ignimbrite, the volcaniclastic member, the Cardones ignimbrite, the Molinos ignimbrite, and the Oxaya ignimbrite (e.g., Wörner et al., 2000; García et al., 2004; van Zalinge et al., 2016). The Lupica Formation, located in the Western Cordillera is thought to be the eastern, more-proximal equivalent of the Oxaya Formation (García et al., 2004). During the mid-late Miocene, ignimbrite volcanism waned, and volcanism in the region was characterized by mafic shield and dome volcanoes (e.g., Wörner et al., 2000).

In the Central Depression, ignimbrites of the Oxaya Formation are overlain by sediments of the mid-Miocene El Diablo Formation. Two members are recognized within the El Diablo Formation (García et al., 2004, and references herein). The Lower Member consists of conglomerates, sandstones, siltstones, and limestones deposited in a low-energy floodplain and lake basin environment. Clasts in the conglomerates are mainly derived from the Oxaya Formation. The Upper Member is composed of layers of gravel predominantly sourced from mid-Miocene andesitic volcanic rocks in the Precordillera and Western Cordillera deposited in a high-energy fluvial environment. The Upper Member is not present north of the Lluta Quebrada (Fig. 1B). The ages of andesitic clasts indicate that the minimum age of the El Diablo Formation is ca. 12 Ma (García et al., 2004).

After emplacement of the Oxaya Formation, contractional deformation generated a series of N-S–trending long-wavelength anticlines in the Precordillera and a narrow fold-and-thrust belt in the Western Cordillera (e.g., Muñoz and Charrier, 1996; Wörner et al., 2000, 2002; García and Hérail, 2005). Deformation inhibited westward transportation of sediments shedding from Andes, which were trapped in two sedimentary basins, the Huaylas and Copaquilla, which formed on the eastern limbs of the Oxaya and Huaylillas anticlines (e.g., Wörner et al., 2002; García and Hérail, 2005). Growth of the Oxaya anticline is estimated to have occurred between ca. 12 and 10 Ma (Wörner et al., 2000, 2002; García and Hérail, 2005), but the exact folding time window for the Huaylillas anticline is not known. The Huaylas and Copaquilla Basins were filled with up to 350 m of late Miocene–Pliocene syn- and postdeformation fluvial, alluvial, and lacustrine sediments, known as the Huaylas Formation (Figs. 1 and 2; e.g., Salas et al., 1966; Wörner et al., 2002; García et al., 2004; García and Hérail, 2005). In the Copaquilla Basin, the Huaylas Formation is typically divided into an Upper Member and a Lower Member (García et al., 2004). The Lower Member consists of a series of gravels, conglomerates, and sandstones in the form of syndeformation growth strata related to the formation of the Oxaya anticline (García and Hérail, 2005). By contrast, the Upper Member consists of horizontal gravels and conglomerates, interpreted as postdeformation deposits (García and Hérail, 2005). In the Huaylas Basin, the Huaylas Formation is composed of three members: the Lower, Middle, and Upper Members (e.g., Salas et al., 1966; García and Hérail, 2005). The Lower Member is characterized by fluvial conglomerates and gravels derived from the east. The Middle Member is a succession of finely stratified claystones, siltstones, sandstones, diatomite, and bentonite that are interbedded with volcanic rocks. The Upper Member is only observed locally and consists of limestones interbedded with siltstones and sandstones. Both the Oxaya and Huaylas Formations are covered by the late Pliocene Lauca ignimbrite, dated at 2.7 Ma (e.g., Wörner et al., 2000; (Figs. 1C and 2).

METHODS

To constrain the deformation history of an ignimbrite using a line-balanced technique, the original ignimbrite surface must first be identified. If any erosion of the surface has occurred, its full extent can be reconstructed by extrapolating between mapped exposures. The internal stratigraphy of the ignimbrite can be used to estimate how much of the surface may have been lost by erosion. Once the original surface of the ignimbrite has been identified, a line-balanced technique can be used to constrain postemplacement deformation and quantify the generation of structural relief growth.

Prior to performing the line-balanced reconstruction, a suitable initial surface slope needs to be identified. The surface slope of an ignimbrite directly after emplacement can be estimated by measuring the ratio of the vertical height between the source and distal deposit limit (H) and the horizontal runout distance (L) (Sparks, 1976; Hayashi and Self, 1992). On average, large ignimbrites have a H/L of 0.02, which corresponds to a surface slope of 1.15° (Sparks, 1976). To further investigate suitable values for original surface slopes of ignimbrites, we collated data on 10 young undeformed extracaldera ignimbrites (Table 1). Slope values were either directly taken from the literature or were determined by overlying existing ignimbrite distribution maps on Google Earth topographic imagery, enabling H/L to be calculated. The results demonstrate that original surface slopes of young undeformed ignimbrites are typically <2°, although some of the older ignimbrites listed in Table 1 have slightly steeper slopes, possibly due to postdeposition deformation.

The results of the line-balanced reconstruction can be used to determine the paleotopography covered by the ignimbrite. However, this requires identification of the base of the ignimbrite and measurement of its full thickness. The internal stratigraphy of the ignimbrite can be then used to confirm the reconstructed paleotopography.

The age difference between the deformed ignimbrite and undeformed overlying deposits

TABLE 1. SURFACE SLOPES OF YOUNG IGNIMBRITES AND THEIR INITIAL SURFACE SLOPES

	Deposit	Age	Average surface slope	Reference
1	The Valley of Ten Thousand Smokes ignimbrite (Alaska, USA)	A.D. 1912	~1.3°	Walker et al. (1980)
2	Minoan ignimbrite (Santorini, Greece)	Late Bronze age (ca. 1650 B.C.)	1–2°	Bond and Sparks (1976)
3	Kurile Lake caldera-forming ignimbrite (KO) (Kamchatka, Russia)	Ca. 7.6 ka	0.5–1.5°	Ponomareva et al. (2004)
4	Ito pyroclastic flow deposit (Aira caldera, Japan)	Ca. 24.5 ka	1–3°	Yokoyama (1974)
5	Youngest Toba Tuff (Indonesia)	Ca. 74 ka	<1°	Aldiss and Ghazali (1984)
6	Zaragoza ignimbrite (Los Potreros caldera, Mexico)	Ca. 100 ka	1–3°	Carrasco-Núñez and Branney (2005)
7	Bishop Tuff (Long Valley caldera, USA)	Ca. 760 ka	1–5°	Wilson and Hildreth (1997)
8	Bandelier Tuff, Pajarito Plateau (Valles caldera, USA)	Ca. 1.4 Ma	2–3°	Smith and Bailey (1966)
9	Huckleberry Ridge tuff, Eastern Snake River Plain (USA)	Ca. 2.05 Ma	~0.5°	Lanphere et al. (2002)
10	Cerro Galan ignimbrite (Argentina)	Ca. 2.08 Ma	0.5–2.5°	Cas et al. (2011)

Note: Data points 1, 2, 4 and 7 are directly from the literature. Other data were found by overlying existing ignimbrite distribution maps on Google Earth topographic imagery, from which H/L was calculated and the mean surface slopes determined.

provides a maximum time constraint for the duration of deformation since ignimbrite emplacement. By combining this duration with the estimated amount of structural relief growth over the time period, local rates of relief growth can be calculated. To date the undeformed volcanic deposits, we used U-Pb zircon geochronology. Zircons were extracted from pumice falls, ash falls, and pyroclastic surge and flow deposits using conventional mineral separation techniques, and individual grains were then handpicked and annealed in a quartz dish in a furnace at 900 °C for 60 h. Representative zircons from each sample were mounted in epoxy resin, polished to expose the grain interiors, and imaged using a Centaurus cathodoluminescence (CL) detector on a Hitachi S3500N scanning electron microscope (SEM) at the University of Bristol. U-Pb zircon analyses were performed at the Natural Environment Research Council Isotope Geosciences Laboratory (NIGL) in Keyworth, UK. The $^{206}Pb/^{238}U$ and $^{207}Pb/^{235}U$ ages were obtained with a Nu Instruments "Nu Plasma" high-resolution multicollector–inductively coupled plasma–mass spectrometer connected to a New Wave Research 193FX excimer laser-ablation system (LA-MC-ICP-MS). Analytical points had a spot size diameter of 35 µm, and up to two points were analyzed in each grain. The standard-sample bracketing technique with primary standard 91500 (1063.6 ± 1.4 Ma; Schoene et al., 2006) and secondary standard Mud Tank (732 Ma; Black and Gulson, 1978) was used to normalize $^{206}Pb/^{238}U$ and $^{207}Pb/^{235}U$ ratios. U-Pb data were reduced with in-house spreadsheets at NIGL and plotted with Isoplot version 4.1 (Ludwig, 2003). Full details about the methodology can be found in Table DR1.[1] In addition, four zircons were analyzed with whole-grain high-precision U-Pb zircon isotope-dilution–thermal ionization mass spectrometry (ID-TIMS), also at NIGL. The method is fully described in van Zalinge et al. (2016).

To determine eruption ages, we used the reproducibility of single $^{206}Pb/^{238}U$ dates that define the youngest coherent population. This was evaluated through calculating weighted mean ages with acceptable mean square weighted deviation (MSWD) values according to the method of Wendt and Carl (1991).

[1]GSA Data Repository Item 2016360, Table DR1: Data reporting template (metadata) for LA-ICP-MS U-Th-Pb data; Table DR2: Results of line-balanced reconstructions; Table DR3: LA-ICP-MS U-Pb zircon geochronology data; Table DR4: ID-TIMS U-Pb zircon geochronology data; Supplemental Text File: Calculations of weighted means $^{206}Pb/^{238}U$ dates, is available at www.geosociety.org/pubs/ft2016.htm, or on request from editing@geosociety.org.

DATA

The Cardones ignimbrite covers a total area of more than 4200 km^2 (García et al., 2004), and in the study area (~1000 km^2), it entirely buries the underlying paleotopography (Figs. 1B, 2, and 3A). Before presenting the results of the line-balanced reconstruction, we: (1) describe the internal stratigraphy of the Cardones ignimbrite; (2) describe the present-day configuration of the Cardones ignimbrite, including thickness, deformation, and its relationship with underlying and overlying lithologies; and (3) identify undeformed lithologies that can be used to constrain the duration of deformation. The data are based on observations from both drill cores and outcrops in the Lluta Quebrada.

The Cardones Ignimbrite: Internal Stratigraphy

Based on drill-core observations, the Cardones ignimbrite consists of two units; their internal structure was described in detail by van Zalinge et al. (2016). The lower unit (Unit 1) is the most extensive, thickest, and best preserved (Fig. 3A). Based on lithologies and textures of lithic and juvenile clasts, four transitional subunits are recognized in Unit 1; these are, from base to top: subunit 1; subunit 2; subunit 3; and subunit 4. Subunit 1 is weakly to moderately welded and contains less than 30% crystals, 1% juvenile clasts, and 2% lithic clasts (mainly granite and andesite). Subunit 2 is moderately welded and contains on average 50% crystals, 3% juvenile clasts, and up to 4% lithic clasts (mainly granite and andesite). Subunit 3 is strongly welded and has similar characteristics to subunit 2, but it only contains 0.2% lithic clasts. Subunit 4 is weakly welded to unwelded and contains on average 40% crystals, 10% juvenile clasts, and 5% lithic clasts (mainly dacite and rhyolite). Welding and compaction as a result of pore-space reduction in pumice and matrix of Unit 1 resulted in an ignimbrite thickness reduction of ~30% (van Zalinge et al., 2016). In particular, the strongly welded subunit 3 contributes ~60% to the thickness reduction. The unwelded top of subunit 4 is considered to be the original surface of Unit 1 and was used in the line-balanced reconstruction.

The Cardones Ignimbrite: Present-Day Configuration

The present-day configuration of the Cardones ignimbrite across the Central Depression, Precordillera, and Huaylas Basin, north of the Lluta Quebrada, is presented in an orogen-perpendicular cross section in Figure 3A. The cross section includes the location of the seven drill cores in the Precordillera (holes 7, 4, 2, 1, 5, 6 and 9, which lie along a NE-SW line spanning the Precordillera from the eastern edge of the Central Depression to the western margin of the Huaylas Basin), as well as the location of the Molinos field section in the Central Depression. The Molinos section is the only easily accessible field location for sampling the Oxaya Formation in the steep northern wall of the Lluta Quebrada (García et al., 2004; van Zalinge et al., 2016).

The Central Depression, West of the Molinos Section

Across the Central Depression, the unwelded top of the Cardones ignimbrite can be clearly recognized in the field, and thus the full thickness of Unit 1 is preserved. West of the Molinos section, only the upper sequence of the Oxaya Formation (i.e., the Oxaya ignimbrite, the Molinos ignimbrite, and the upper part of the Cardones ignimbrite) crops out in the Lluta Quebrada (Fig. 3B). The sequence, including the upper surface of the Cardones ignimbrite, dips westward with an average angle of 1.3°; no overt deformation can be recognized.

The Central Depression, from the Molinos Section to Hole 7

Between the Molinos section and the Ausipar thrust, both the Oxaya Formation and the top of the underlying Azapa Formation crop out in the Lluta Valley. The whole exposed sequence, including the surface of the Cardones ignimbrite, has an average westward dip of ~4°. The Ausipar thrust cuts and offsets the top of the Azapa Formation and the Poconchile ignimbrite with an estimated vertical throw of ~200 m and horizontal shortening of ~240 m (Fig. 3C). The thrust has a tip-point just above the Poconchile ignimbrite and just below the Cardones ignimbrite (García et al., 2004; García and Hérail, 2005). Consequently, the Cardones ignimbrite is folded into an ~2-km-wide fault propagation flexure dipping up to ~20° to the west. Taking this small fold into account, the average surface slope for the Cardones ignimbrite is 5.5° between the Molinos section and hole 7. The Cardones ignimbrite gradually thickens toward the east, with a thickness of ~300 m near the Molinos section and 470 m in hole 7 (Table 2). The Azapa Formation has a thickness greater than 250 m in the Central Depression (the base of the formation is buried, and the full thickness is not observed).

Precordillera, from Hole 7 to Hole 9

The seven drill holes (7, 4, 2, 1, 5, 6, and 9) lie along a NE-SW line through the Precordillera from the eastern edge of the Central Depression

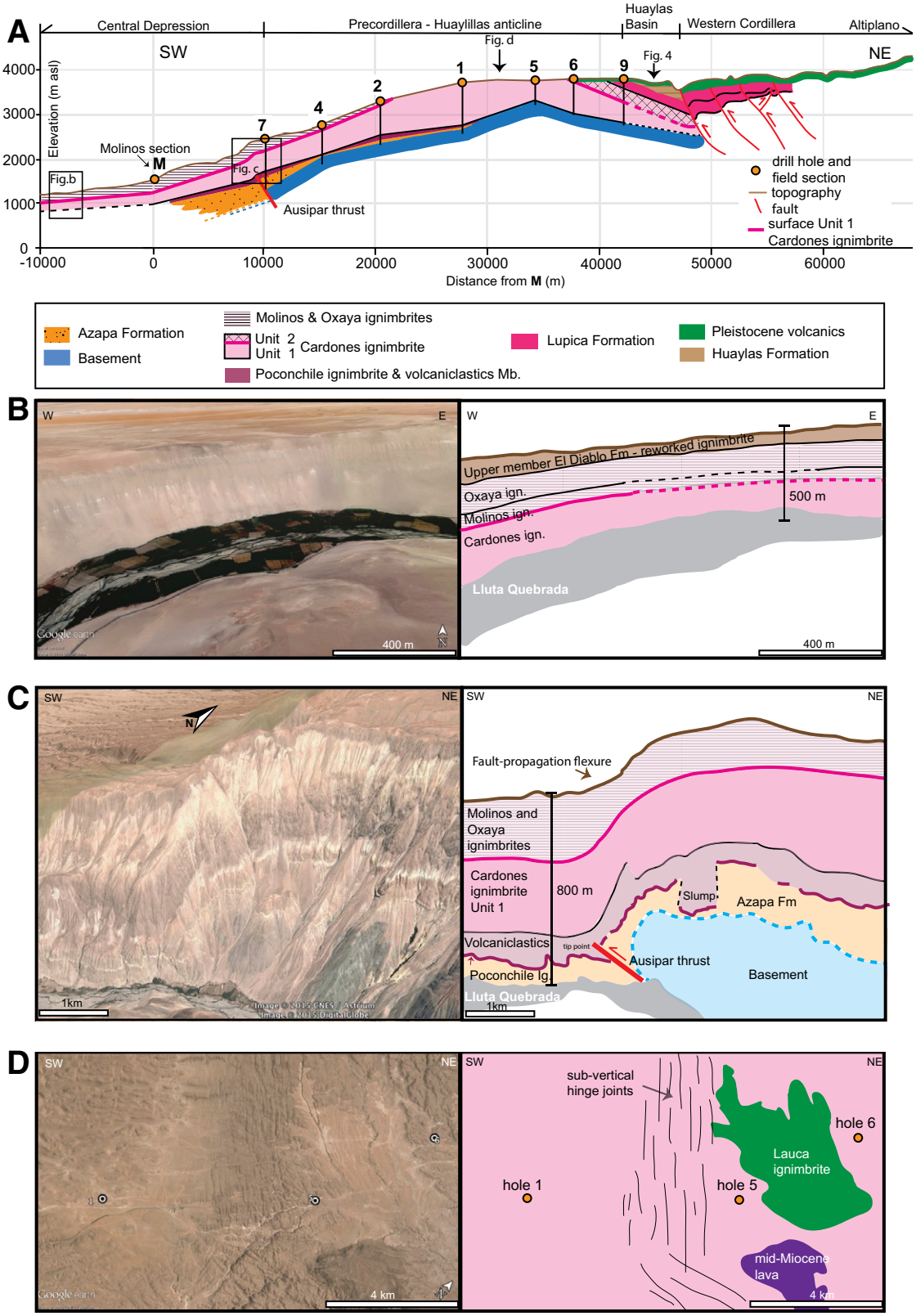

Figure 3. (A) SW-NE cross section of the Western Andean Slope based upon field observations and drill-core data presented in van Zalinge et al. (2016). The cross section east of hole 9 is based on the map of García et al. (2004), and fault structures are based on observations east of the Copaquilla Basin by Muñoz and Charrier (1996); asl—above sea level. (B–D) Google Earth™ views and line-drawn interpretations of key structural and stratigraphic relationships. (B) Undeformed upper section of the Oxaya Formation in the northern wall of the Lluta Quebrada, Central Depression; (C) Ausipar thrust in the northern wall of the Lluta Quebrada; (D) a series of subvertical NW-SE–trending fractures along the hinge of the Huaylillas anticline.

TABLE 2. THICKNESS OF UNIT 1 AND SUBUNITS IN UNIT 1 OF THE CARDONES IGNIMBRITE

Location	Latitude (°S)	Longitude (°W)	Unit 1 (m)	Sub 1 (m)	Sub 2 (m)	Sub 3 (m)	Sub 4 (m)
M	18°22′01″	69°57′14″	~300	Unknown	Unknown	Unknown	Unknown
7	18°17′59″	69°53′12″	470	0	110	250	110
4	18°16′11″	69°50′47″	580	0	150	330	100
2	18°14′15″	69°48′39″	690	0	170	410	110
1	18°11′11″	69°45′46″	**1190**	130	200	550	**310**
5	18°8′53″	69°43′01″	**770**	0	200	**400**	**170**
6	18°6′50″	69°42′14″	730	0	250	350	130
9	18°4′59″	69°40′32″	455	0	30	215	210

Note: Modified from van Zalinge et al. (2016). Numbers in bold are reconstructed thicknesses.

to the western margin of the Huaylas Basin. Here, the Cardones ignimbrite is gently folded by the Huaylillas anticline (Fig. 3A), the hinge of which (between holes 1 and 5) is characterized by a series of subvertical NW-SE–trending (azimuth: 138°) fractures (Fig. 3D). Table 2 presents the thicknesses of the different subunits in Unit 1 in each hole. Subunit 4 and the top part of subunit 3 have been eroded from holes 1 and 5, which are located in the anticlinal hinge zone. The full thickness of the Cardones ignimbrite is preserved on the eastern and western limbs of the anticline. The upper surface has a slope between 5.5° and 6.1° (with an average of 5.7°) on the western limb and a slope of 5.7° on the eastern limb. Furthermore, the basal subunits 1 and 2 are laterally discontinuous, as subunit 1 is only present in drill hole 1, and subunit 2 is very thin in hole 9. In the eastern part of the Precordillera (east of hole 1), the Azapa Formation and the oldest members of the Oxaya Formation are missing, and thus the Cardones ignimbrite directly overlies the Jurassic–Paleocene basement. The Azapa Formation overlies the basement with a thickness of less than 50 m in holes 1 and 2 and is absent in hole 4. Note that the Azapa Formation is significantly thicker to the west (260 m in hole 7 and >250 m in the Central Depression).

Huaylas Basin: Identification of Undeformed Deposits

Lying to the east of the Huaylillas anticline, the Huaylas Basin is an ~6-km-wide and ~20-km-long N-S–trending depression. The basin is filled with Huaylas Formation sediments, which lie above the Oxaya Formation and are partly covered by the Lauca ignimbrite (Fig. 4). Hole 9 was drilled on the western edge of the Huaylas Basin (Figs. 1C and 3) and sampled an ~90-m-thick sedimentary sequence overlying a pyroclastic sequence (including the Cardones ignimbrite). A detailed stratigraphic log of the top of hole 9 is presented in Figure 5A. The lower ~50 m section of the sedimentary interval is characterized by polymict, poorly sorted, matrix-supported conglomerates. The clasts are mainly angular to subrounded porphyritic andesites and dacites hosted in a reddish-brown sandy matrix. The clasts are commonly altered and range from a few millimeters to tens of centimeters in size. The poorly sorted, immature nature of the clasts indicates that they were locally sourced and deposited by debris flows. These conglomerates are unconformably overlain by a 40-m-thick interval of well-sorted, horizontal, finely bedded claystones, siltstones,

Figure 4. North-looking view of the Huaylas Basin where the Attane Quebrada dissects the Huaylas Formation. The Huaylas Formation is covered by the late Pliocene Lauca ignimbrite and Quaternary volcanic deposits.

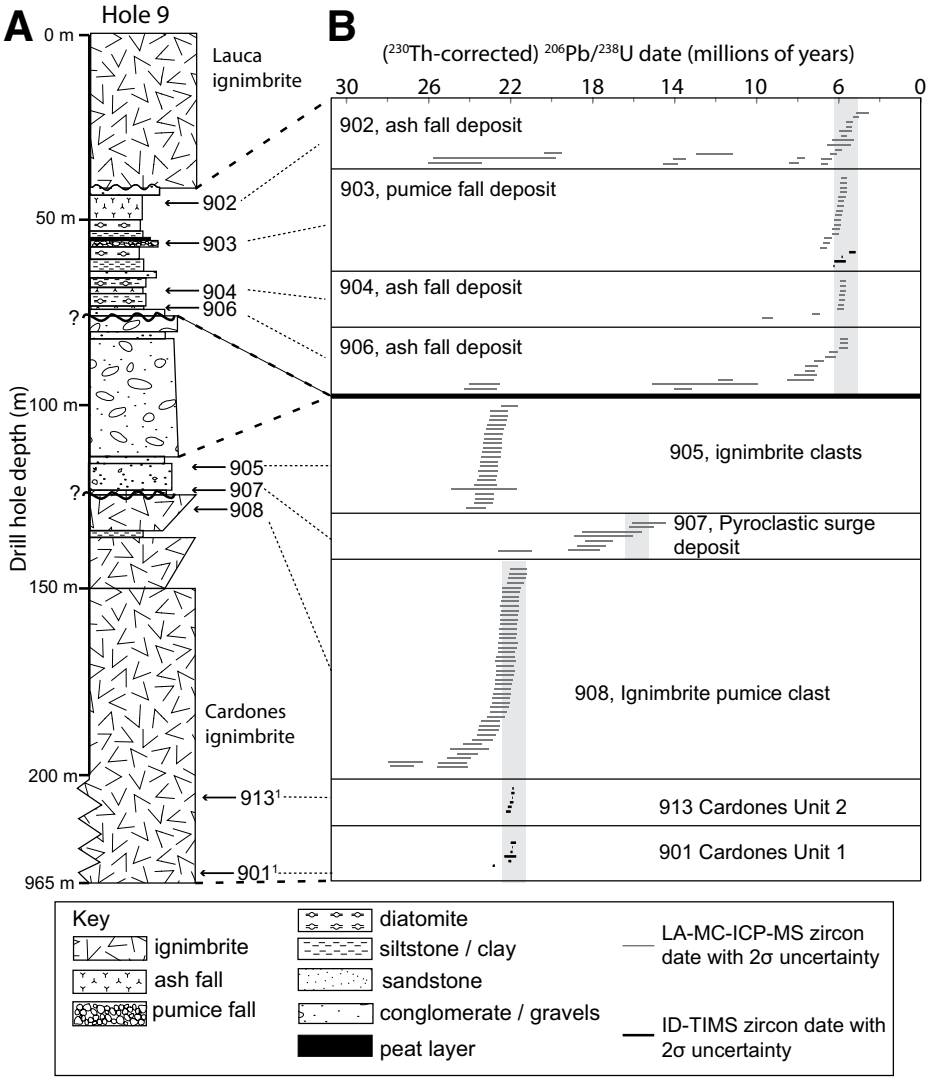

Figure 5. (A) Stratigraphic column of the Huaylas Formation in hole 9, indicating sample locations for U-Pb geochronology. (B) Laser-ablation–multicollector–inductively coupled plasma–mass spectrometry (LA-MC-ICP-MS) and isotope-dilution–thermal ionization mass spectrometry (ID-TIMS) ^{230}Th-corrected ^{206}Pb/^{238}U dates for hole 9. 1—Dates from sample 901 and 913 from van Zalinge et al. (2016).

sandstones, diatomite, and organic-rich layers interbedded with minor volcanic ash and pumice horizons, indicating a low-energy lacustrine environment. Similar lacustrine deposits have been observed in the field at the Attane Quebrada to the east of hole 9 (Fig. 4). There was no evidence in drill hole 9 or in the field that these lacustrine deposits are deformed.

RESULTS

Reconstruction of the Ignimbrite Surface

Unit 1 of the Cardones ignimbrite is partly eroded in the hinge zone of the Huaylillas anticline, but it is well preserved in both anticlinal limbs. We reconstructed the original thickness of Unit 1 by extrapolating the present-day 5.7° surface slope of each limb toward the hinge (Fig. 6A). This allowed us to estimate the original thickness of the Cardones ignimbrite in hole 1 (1190 m), hole 5 (770 m), and the hinge of the Huaylillas anticline. Subtraction of the reconstructed thickness from the observed thickness indicates that as much as 560 m of Cardones ignimbrite thickness has been eroded from the fold hinge zone between holes 2 and 6 (Fig. 6A; Table DR2). This means that the overlying Molinos and Oxaya ignimbrites must also have been eroded. Furthermore, we extended the upper surface of Unit 1 eastward to point "E" where the Western Cordillera begins and the cross-section line intersects a thrust fault mapped by García et al. (2004). We define this point as the eastern edge of the anticline (Figs. 3 and 6).

Line-Balanced Reconstruction of the Cardones Ignimbrite

The reconstructed surface of Unit 1 in the Cardones ignimbrite was used to implement the line-balanced reconstruction method (Fig. 6). First, we considered upper and lower bounds on the initial surface slope of the top of Unit 1. Observations indicate that most undeformed young ignimbrites have initial surface slopes between 1° and 2° (Table 1). Reconstructions using these bounding slope values, however, produced features inconsistent with the geological observations and enabled us to reduce the uncertainty in our estimate of the initial slope. Surface slopes exceeding 1.76° placed the eastern end of the reconstructed profile above the present-day surface, yet there is no evidence for significant subsidence and eastward tilting of the area (e.g., Isacks, 1988; García and Hérail, 2005; Farías et al., 2005; Jordan et al., 2010). Thus, our results suggest that the original surface slope was <1.8°. A slope of <1.2° creates two problems for reconstructions. First, the initial slope would be less than the slope of the Cardones ignimbrite in the Central Depression, which we assume to be untilted/undeformed. Second, the top of the Azapa Formation west of hole 7 would dip to the west, when we know from imbricated clasts that sediments were transported from the northeast (García et al., 2004, and references therein). We thus choose to present reconstructions for 1.5° (Fig. 6B) and assume an uncertainty of 0.3° for inferences that are made from the reconstructions of tilting and uplift.

We chose the Molinos section (location M) as the western pinpoint for the line-balanced reconstruction because no overt deformation has been observed west of the Molinos section. Since we do not have a well-determined absolute pre-Cardones paleoelevation for M, all calculated "uplift" is reported as structural relief growth. Thus, all determined paleoelevations are relative to M, as we do not know how much the forearc may have uplifted and subsided as an isostatic response to contractional deformation and ignimbrite burial. The results of the reconstructions are presented in Table 3 and Figure 6, and the full data set can be found in Table DR2.

Posteruptive Deformation

The structural relief growth related to folding was calculated under the assumption that all folding occurred due to buckling, with the elevation of point E being fixed. All other relief growth measured at point E was assigned to

TABLE 3. RESULTS OF THE LINE-BALANCED RECONSTRUCTION, USING THE BOUNDING SURFACE SLOPES OF 1.2° AND 1.8°

Location	M	7	4	2	1	Hinge	5	6	9	E
Ground distance from M (m)	0	9850	15,240	20,410	27,770	31,616	34,200	37,680	42,220	48,000
1.2° surface slope—Relief growth										
Relief growth folding (m)	0	640	980	1375	1880	2140	1800	1350	755	0
Relief growth tilting (m)	0	95	150	200	275	310	340	370	415	475
Total relief growth (m)	0	735	1130	1575	2150	2450	2140	1720	1170	475
1.8° surface slope—Relief growth										
Relief growth folding (m)	0	640	980	1375	1880	2140	1800	1350	755	0
Relief growth tilting (m)	0	–5	–10	–15	–20	–20	–20	–25	–30	–30
Total relief growth (m)	0	635	970	1360	1860	2120	1780	1325	725	–30
Relief growth 1.5° ± 0.3 surface slope	0	685 ±50	1050 ±80	1470 ±110	2005 ±145	2285 ±165	1960 ±180	1525 ±200	950 ±225	225 ±255
Elevation of the base of the Cardones ignimbrites—Paleotopography pre–21.9 Ma										
1.5° ± 0.3 surface slope	900	995 ±50	1025 ±80	1050 ±110	740 ±145		1340 ±180	1470 ±200	1860 ±225	

Note: "Hinge" refers to the reconstructed hinge of the Huaylillas anticline between holes 1 and 5. The elevation of the base of the Cardones ignimbrite indicates the elevation of the paleotopography prior to eruption of the Cardones ignimbrite. Note that this elevation is relative to that of the Molinos section (M), for which the paleoelevation at 21.9 Ma is unknown. The elevation of M was fixed during the line-balanced reconstructions at its present-day elevation of 900 m.

tilting (Fig. 6C). Assuming no erosion, a surface slope of 1.5° ± 0.3° gives a maximum relief generation of 2285 ± 165 m along the anticlinal hinge. Over a distance of ~50 km (from the eastern edge of the Central Depression to the easternmost edge of the Precordillera), the amount of shortening is 220 ± 10 m, and therefore the total strain between M and E is ~4×10^{-3}. The amount of relief generated by westward tilting depends on the distance from M (Table 3). At the easternmost point E, the maximum relief generation related to tilting is 225 ± 255 m (Fig. 6B). The Cardones ignimbrite has experienced up to ~560 m of erosion at the hinge of the anticline during and/or after deformation. By subtracting this erosion from 2285 ± 165 m, we calculate a maximum relief growth after deposition of the Cardones ignimbrite of 1725 ± 165 m. Although the Oxaya and Molinos ignimbrites have also been removed by erosion in the hinge zone, they do not contribute to our estimates of structural relief growth because the Cardones ignimbrite is used as the paleomarker.

Pre-Eruptive Paleotopography

The base of the Cardones ignimbrite in the reconstructed sections in Figure 6B represents the paleotopography prior to ignimbrite emplacement. Key features of this paleotopography are: (1) a nearly flat surface west of hole 1, with a westward slope of 0.4° ± 0.3°; (2) a paleodepression 450 ± 150 m deep at hole 1; and (3) a surface dipping 3.7° ± 0.3° east of hole 1 (Fig. 6B). Our line-balanced reconstructions imply that the eastern part of the Precordillera had a paleoelevation 960 ± 225 m higher than the eastern part of the Central Depression prior to emplacement of the Cardones ignimbrite. This reconstructed paleotopography is supported by the presence of subunit 1 in paleolows and the absence of thick basal subunits on paleohighs (Fig. 6). The thickness variations in the Cardones ignimbrite with the ponding of lower units in topographic lows, the absence of Azapa sediments east of hole 1, and the thickening of the Azapa sediments to the east toward the Central Depression all indicate that by 21.9 Ma, the Precordillera already had a quite rugged topography, which was infilled by the Cardones ignimbrite.

Finally, we note that in our reconstruction, the top surface of the Azapa Formation west of hole 4 has an apparent eastward dip of 1.2° ± 0.3°, which is inconsistent with sediment transport from the northeast. We attribute this observation to erosion, which has cut down through the Azapa Formation, leaving a surface that does not represent a single time horizon. Evidence for erosion includes the absence of the Azapa Formation in hole 4 and the absence of the overlying Poconchile ignimbrite in both holes 4 and 1 (van Zalinge et al., 2016). Specifically, the Poconchile ignimbrite should be expected in hole 1, where it would have ponded in the paleodepression. Its absence suggests significant erosion of the lower Oxaya and Azapa Formations in hole 1.

U-Pb Geochronology of the Oxaya and Huaylas Formations

In order to place constraints on the timing of deformation, we selected samples from hole 9 for U-Pb zircon geochronology, including three samples from the pyroclastic sequence (905, 907, and 908) overlying the Cardones ignimbrite and four volcanic intervals (902, 903, 904, and 906) in the flat-lying undeformed lake sediments. Figure 7 shows the ID-TIMS and LA-MC-ICP-MS results for all ^{230}Th-corrected ^{206}Pb/^{238}U dates alongside the stratigraphy of hole 9. All ages are reported at the 2σ confidence level. A minor proportion (for each sample $n < 4$) is older than 30 Ma, and these are not shown in Figure 5B or included in the discussion, because we interpret them as resulting from the incorporation of xenocrystic material. The full data set along with calculations of weighted mean ages for the youngest coherent zircon population in each sample can be found in Tables DR3–DR4 and the Supplemental Text File. After excluding ages older than 30 Ma, the samples still give a range of ^{206}Pb/^{238}U ages that exceeds the 2σ analytical uncertainty. This range typically varies from 0.5 to a few million years and may result from magmatic processes (e.g., prolonged crystal growth, incorporation of antecrysts), entrainment of zircon during eruption, transport and sedimentation, or postdepositional Pb loss (Bowring et al., 2006).

Samples 908 and 907, collected from the pyroclastic sequence above the Cardones ignimbrite, show a decrease in age upward in the stratigraphy, with weighted mean ages of 22.179 ± 0.092 Ma and 17.95 ± 0.37 Ma, respectively. Sample 905, collected above these two samples, but still within the pyroclastic sequence, gives a weighted mean age of 22.99 ± 0.11 Ma, i.e., significantly older than sample 907. We therefore suggest sample 905 derives from a large ignimbrite clast that was difficult to identify in the one-dimensional drill core, rather than an in situ deposit. Nevertheless, all ages are consistent with previously published data for the Oxaya and Lupica Formations (e.g., García et al., 2004).

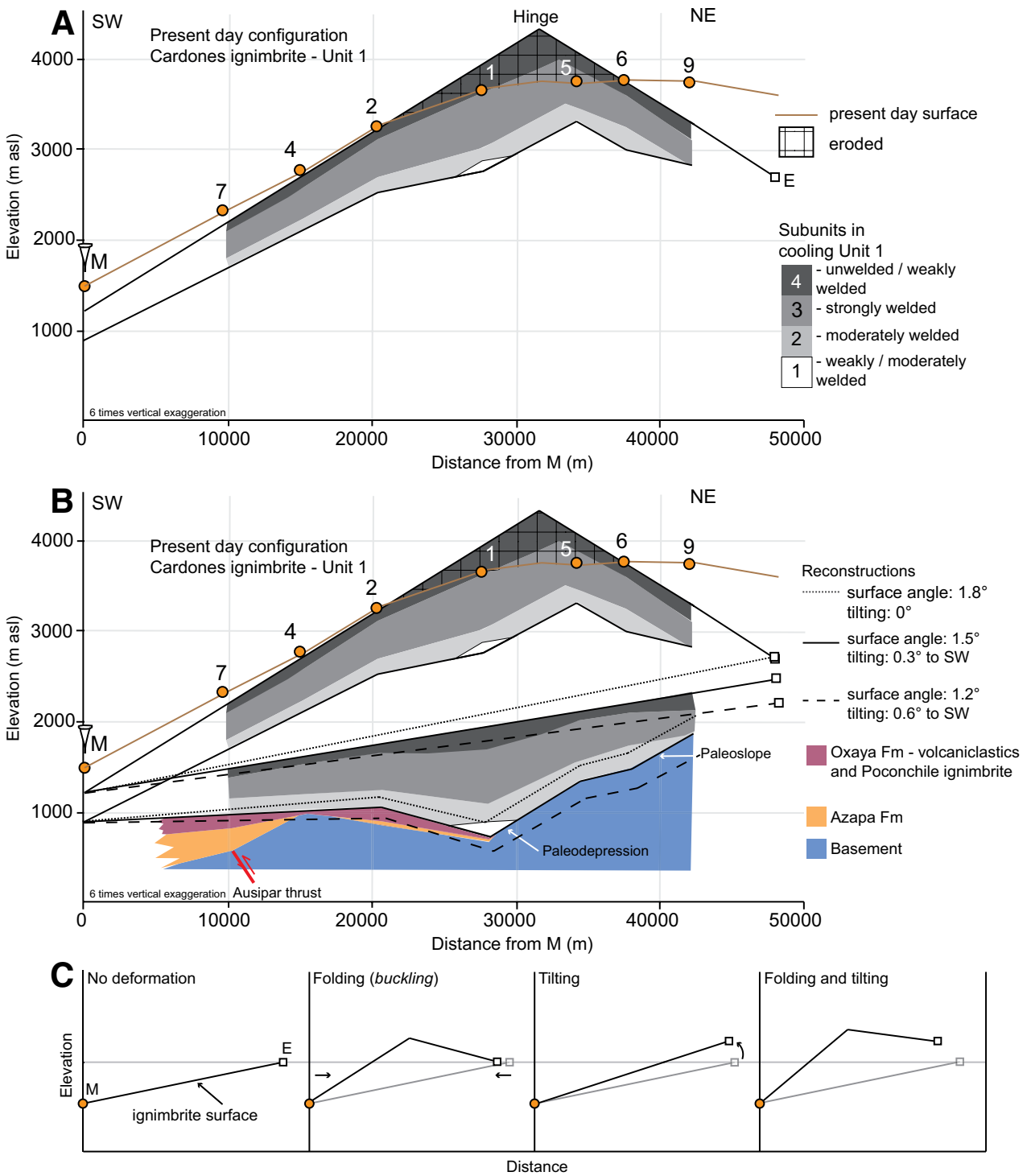

Figure 6. (A) Present-day configuration of the Cardones ignimbrite between the Molinos section (M) and the end of the anticline (E), with the reconstructed surface of Unit 1. Note that the subunits in Unit 1 are indicated by different shades of gray; asl—above sea level. (B) Three reconstructions with bounding (1.2° and 1.8°) and average (1.5°) initial surface slopes plotted below the present-day configuration. Subunits within Unit 1 and underlying lithologies of the Cardones ignimbrite are indicated in the reconstruction with a 1.5° surface slope. Note that the base of the Cardones ignimbrite in the line-balanced reconstructions represents the restored paleotopography. (C) Illustrations showing how the amount of shortening and uplift related to folding and tilting were calculated. Note that the elevation of E is fixed during folding.

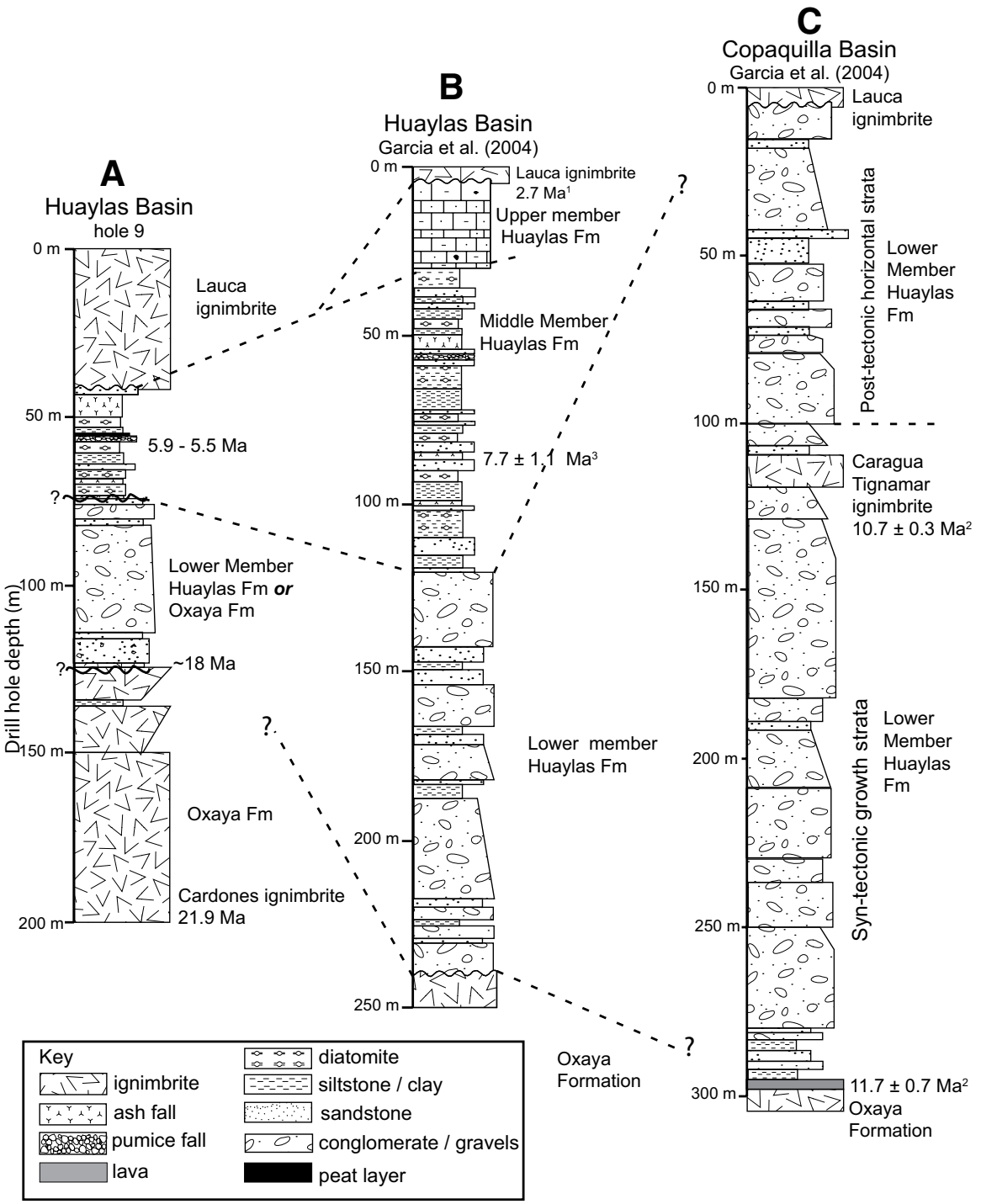

Figure 7. Stratigraphic correlation of the Huaylas Formation in: (A) hole 9 (this study); (B) the Huaylas Basin (stratigraphy based on observations in the Attane Quebrada by García et al., 2004); (C) the Copaquilla Basin, west of the Oxaya anticline (stratigraphy based on descriptions by García et al., 2004; García and Hérail, 2005). 1—age from Wörner et al. (2000a); 2—ages from García and Hérail (2005); 3—age from García et al. (2004).

LA-MC-ICP-MS analyses of samples collected from the lacustrine deposits give significantly younger weighted mean ages than those of the Oxaya Formation. From base to top, these are: 5.80 ± 0.11 Ma (906); 5.894 ± 0.053 Ma (904); 5.909 ± 0.075 Ma (903); and 5.69 ± 0.15 Ma (902). Four ID-TIMS $^{206}Pb/^{238}U$ dates for sample 903 range from 5.396 ± 0.160 Ma to 6.296 ± 0.025 Ma (Table DR4), but these do not give a statistically valid weighted mean age. Combined, these data constrain deposition of the flat-laying lake deposits to ca. 5.9–5.5 Ma, i.e., the latest stage of the Miocene.

Comparison of our results with previous descriptions of the Huaylas Formation in the Huaylas Basin (Fig. 7B; García et al., 2004) lead us to correlate the lacustrine sequence with the Middle Member of the Huaylas Formation. The poorly sorted immature conglomerates that we have constrained between ca. 18 and 6 Ma could be correlated to the syndeformational Lower Member of the Huaylas Formation in the Copaquilla and Huaylas Basins. However, the limitations of one-dimensional drill-core observations do not allow us to identify whether these conglomerates were deposited as a growth stratum related to the formation of the Huaylillas anticline. Alternatively, the volcanic-rich nature of the clasts may imply that these deposits were formed from lahars and could be part of the Oxaya/Lupica Formation. Nevertheless, the lack of ignimbrite clasts favors the interpretation that they are equivalent to the conglomerates of the Lower Member of the Huaylas Formation sourced from the east.

The Oxaya and Molinos ignimbrites are both missing in hole 9, and there is a potential hiatus in deposition of up to 12 m.y. Consequently, we propose at least one, and possibly more, erosional unconformities between the top of the Cardones ignimbrite and the base of the lacustrine deposits (Fig. 5). Figure 7 shows the temporal relationship between the Huaylas Formation in the Huaylas Basin and the Copaquilla Basin. The onset of gravel sedimentation in the Copaquilla Basin is constrained to ca. 12 Ma, whereas the onset of sedimentation in the Huaylas Formation is unclear. Our data suggest that infill of the Huaylas Basin could have commenced up to 6 m.y. earlier, after ca. 18 Ma. The 10.7 Ma Caragua Tignamar ignimbrite marks the end of the syntectonic growth strata in the Copaquilla Basin (Wörner et al., 2000; García and Hérail, 2005), after which minor sedimentation occurred. Data from the Huaylas Basin suggest a change to lacustrine sedimentation conditions around 6 Ma, but such a change is not observed in the Copaquilla Basin. However, the onset of lacustrine sedimentation in the late Miocene is consistent with dating of ashes intercalated with lacustrine Lauca Formation sediments in the Lauca Basin, east of the Belen Ridge (Fig. 1B; Kött et al., 1995; Gaupp et al. 1999).

DISCUSSION

The large-volume Oxaya Formation ignimbrites, including the 21.9 Ma Cardones ignimbrite, inundated and buried large parts of northernmost Chile (18°S–18.5°S) in the early Miocene. Despite significant postemplacement deformation, some of these ignimbrites are exceptionally well preserved and enable the history of structural relief and topography on the Western Andean Slope to be elucidated. By combining a line-balanced reconstruction of the surface of the Cardones ignimbrite with detailed stratigraphic analysis and U-Pb zircon geochronology, we show that significant relief generation and fluvial incision on the Western Andean Slope commenced before ca. 22.7 Ma and that the main deformation ceased before 6 Ma (Fig. 8).

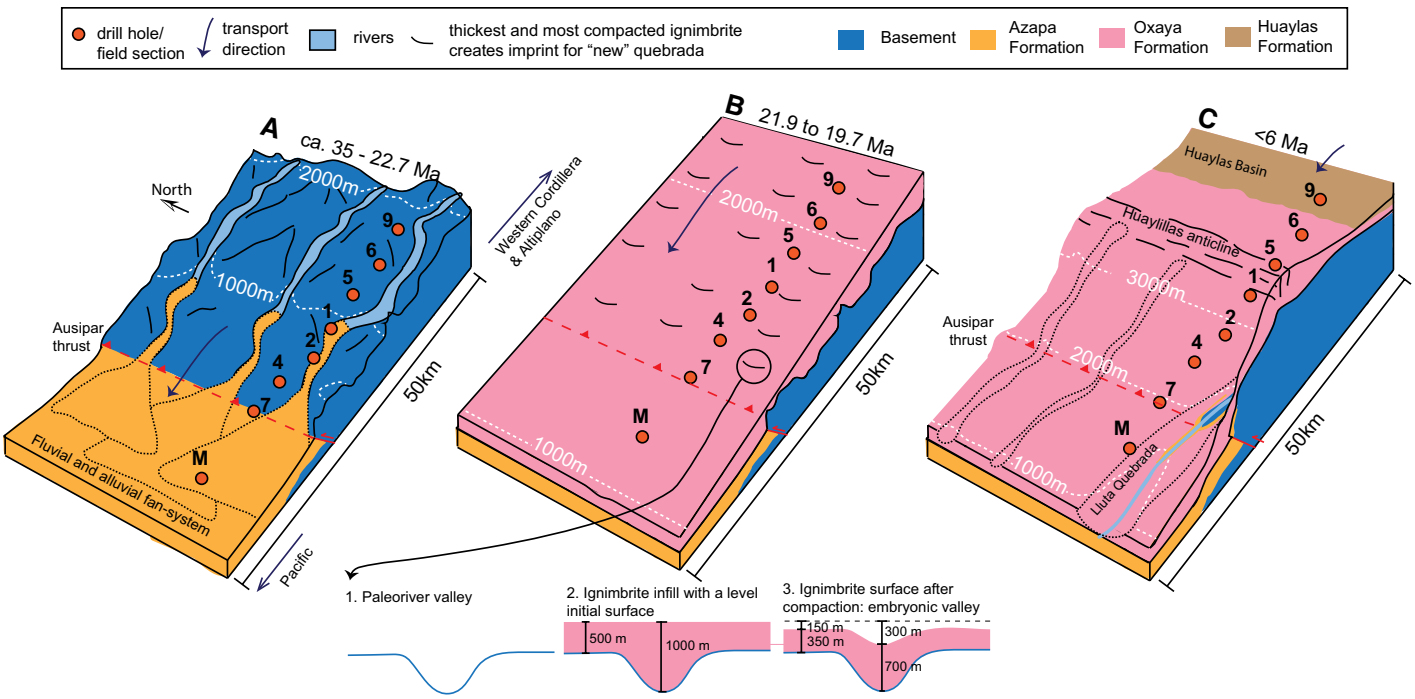

Figure 8. Schematic illustration of the development of the Western Andean Slope in northernmost Chile between >22.7 Ma and ca. 6 Ma. (A) Between ca. 35 Ma and >22.7 Ma, development of a paleoslope was characterized by structural relief growth in the east and the creation and infilling of accommodation space in the west. (B) In the early Miocene (21.9–19.7 Ma), large-volume ignimbrites of the Oxaya Formation entirely covered the preexisting topography, forming a planar surface with a gentle slope of 1.5° ± 0.3°. Welding compaction was greatest where the ignimbrite was thickest (i.e., infilled valleys), creating an imprint in the topography that controlled the location of future river incision. (C) By 6 Ma, this gentle surface slope had been deformed into the Huaylillas anticline and was incised by the Lluta River. On the eastern limb of the anticline, accommodation space (the Huaylas Basin) was created and infilled by sediments of the Huaylas Formation.

Pre–21.9 Ma Deformation and Structural Relief Growth

The reconstructed pre-eruptive paleotopography reveals the existence of a paleoslope on the western flank of the Central Andes prior to 21.9 Ma. This slope dipped 3.7° ± 0.3° westward and, in the eastern Precordillera, reached an elevation up to 960 ± 225 m higher than the eastern margin of the Central Depression. In the eastern Precordillera, this paleosurface was characterized by exhumed basement lithologies (Figs. 3 and 6). In the western Precordillera, the basement dipped westward with an apparent slope of 0.4° ± 0.3° and was unconformably overlain by coarse Azapa sediments that thickened to the west. We suggest that this pre–21.9 Ma paleotopography reflects contemporaneous structural relief growth and erosion in the Precordillera and the creation of accommodation space and sedimentation in the Central Depression, much as is seen in the region today (Fig. 8A).

Our work concurs with previous interpretations that deformation prior to the early Miocene ignimbrite flare-up included an episode of thrusting along the Ausipar thrust, which uplifted the Precordillera and created accommodation space in the Central Depression (e.g., Muñoz and Charrier, 1996; Wörner et al., 2002; García and Hérail, 2005; Charrier et al., 2013). This uplift resulted in erosion of both the Precordillera and Western Cordillera and deposition of a thick sequence of coarse clastic sediments (the Azapa Formation) in the Central Depression (Fig. 8A). Wörner et al. (2002) suggested that these sediments were sourced from the western flank of a proto-Altiplano before 22.7 Ma (the age of the Poconchile ignimbrite, which directly overlies the Azapa Formation; Fig. 2), and our observations are consistent with this interpretation. Consequently, we suggest that our reconstructed paleoslope (Fig. 8A) reflects initial growth of a proto–Western Andean Slope in the study area. In order to put better time constraints on the development of this slope, we refer to a provenance study of the Azapa Formation performed by Wotzlaw et al. (2011). This study showed that detrital zircons from the Azapa Formation were mostly Paleocene–Cretaceous (60–80 Ma) in age, but included some Eocene (35–50 Ma) material. Consequently, deposition of the Azapa Formation, and therefore initial growth of a proto–Western Andean Slope, can be constrained to between ca. 35 and 22.7 Ma (Fig. 8A).

The line-balanced reconstruction (Fig. 6B) suggests the presence of a paleodepression 450 ± 150 m deep near hole 1, which was subsequently infilled by the Cardones ignimbrite. We interpret this depression to be a river valley and propose, following the principles described in Montgomery and Brandon (2002), that river incision in the Precordillera at this time occurred as a response to exhumation and uplift of the paleo–Western Andean Slope (Figs. 6B and 8A).

Post–21.9 Ma Deformation and Structural Relief Growth

Geological structures observed in the field, such as the Ausipar thrust and the Huaylillas anticline, together with our line-balanced reconstruction indicate that the study area experienced significant structural relief growth after eruption of the Oxaya Formation ignimbrites. Whether this relief generation was a continuation of the deformation that occurred prior to 21.9 Ma, or was a separate deformation event, is unclear from our results. Nevertheless, field observations and satellite imagery of the Ausipar thrust (Fig. 3C) suggest that the latest phase of movement on the structure occurred after emplacement of the 19.7 Ma Oxaya ignimbrite. Furthermore, the entire Oxaya Formation is clearly folded. We therefore conclude that after emplacement of the Oxaya Formation, the study area was faulted, folded, and tilted, resulting in the generation of up to 1725 ± 165 m of structural relief and E-W shortening of 220 ± 10 m in the present-day Precordillera, north of the Lluta Quebrada. This result is consistent with the 1700-m-deep incision observed in the Lluta Quebrada (García et al., 2011) with growth of the fold crest compensated by incision of the river. We note that this estimate assumes that the upper surface of the Cardones ignimbrite was planar and does not account for changes in relief related to welding compaction. With compaction estimated at a 30% reduction in thickness (van Zalinge et al., 2016), the relief could have been a few tens of meters lower in the area of greatest original thickness. This effect would slightly increase the estimate of structural relief growth during contractional deformation.

If erosion of the hinge of the Huaylillas anticline had not occurred, structural relief generation could have been as much as 2285 ± 165 m. Using this result, we calculated the fold amplitude by subtracting the tilt-related uplift. This gives a fold amplitude of 2140 m, which is independent of the assumed initial surface slope (Table 3). At least 90% and as much as 100% of the structural relief generation at the hinge of the anticline can be assigned to folding. The remaining 0%–10% of relief generation is attributed to westward tilting of the Precordillera. We calculated that the Precordillera experienced 0.3° ± 0.3° of westward tilting, which, over a distance of ~50 km, results in uplift of 225 ± 255 m on the eastern edge of the Precordillera (Table 3). In the following section, the timing and folding intensity of the Huaylillas anticline with respect to the Oxaya anticline are discussed in more detail.

Landscape Evolution Related to Ignimbrite Emplacement and Anticline Formation

We have already presented evidence that, prior to ignimbrite emplacement at 21.9 Ma, the Precordillera dipped 3.7° ± 0.3° to the west and was cut by a paleovalley 450 ± 150 m deep. In this section, we will further argue that a valley in the location of the present-day Lluta Quebrada started to incise directly after emplacement of the early Miocene ignimbrites. This interpretation differs from those of Wörner et al. (2002) and García and Hérail (2005), who inferred that incision of the Lluta Quebrada commenced after ca. 12 Ma in response to anticline formation. Here, we discuss further how the landscape responded to inundation by the ignimbrites and formation of the anticlines.

First, any pre-eruptive river system would have been buried by the ignimbrite. Once surface waters were able to establish a new channel network, this river system would have been out of equilibrium because the ignimbrite had changed the surface profile. Equilibrium river profiles are typically concave (up), where the channel slope decreases with distance downstream. By contrast, ignimbrites are generally deposited with approximately constant slopes (Table 1), and thus the initial postemplacement river profiles are too shallow in upstream regions and too steep in downstream regions. The Oxaya Formation ignimbrites are in general thickest in the Precordillera and thin toward the Pacific. Consequently, the source of a river in the east would have increased in elevation relative to its base level in the west. This change would have perturbed the fluvial drainage system, causing it to incise predominantly in the Precordillera in order to reestablish an equilibrium profile. Evidence from very young ignimbrites (e.g., Wilson, 1991) shows that posteruption incision tends to occur most rapidly into the unwelded top of an ignimbrite (within a few years or decades), but then slows down when it reaches the strongly welded ignimbrite beneath.

The second major effect of ignimbrites on landscape evolution relates to welding compaction. The pre–21.9 Ma paleovalley (Fig. 6B) is located in a similar location to the present-day Lluta Quebrada. When large-volume ignimbrites are first emplaced, they infill topography with a level upper surface. However, during welding, the compaction is greatest where the ignimbrite is thickest (e.g., infilled paleovalleys), creating an embryonic topography that controls the location of future river incision (Fig. 8B). In their

study, van Zalinge et al. (2016) calculated that compaction of the Cardones ignimbrite reduced its thickness by about ~30%. For example, an ~1000-m-thick deposit in a paleovalley would lose ~300 m of thickness as a result of compaction, whereas an ~500-m-thick deposit on a paleohigh would lose 150 m of its initial thickness (Fig. 8B). Thus, a 150-m-deep embryonic depression would be formed over the pre-eruption valley, enabling the pre-eruption drainage to be reestablished. Infilling of pre-eruption valleys by ignimbrites and re-exhumation of these ignimbrites to form valleys in approximately the same place are commonly observed phenomena (e.g., Sparks, 1975; Myers, 1976). These arguments suggest that formation of the Lluta Quebrada began prior to folding.

We now consider the evolution of the landscape related to formation of the anticlines and explore the effect of the landscape on folding. Previous studies attributed growth of the Oxaya anticline to an ~2 m.y. time window in the middle Miocene using age constraints from the Huaylas and El Diablo Formations (Wörner et al., 2000, 2002; García and Hérail, 2005). The lower part of the Huaylas Formation in the Copaquilla Basin is defined by growth strata related to formation of the Oxaya anticline (Fig. 7C). A folded lava flow that overlies the Oxaya ignimbrite but underlies the growth strata of the Huaylas Formation was dated at 11.7 ± 0.7 Ma (García and Hérail, 2005), suggesting that folding must have started after deposition of this lava. The end of folding of the anticline is constrained by the flat-lying 10.7 ± 0.3 Ma Tignamar ignimbrite (Wörner et al., 2002; García and Hérail, 2005) that overlies growth strata in the Huaylas Formation (Fig. 7). The onset of folding determined from the Copaquilla Basin is compatible with the ca. 12 Ma minimum age of the Upper Member of the El Diablo Formation west of the Oxaya anticline (García et al., 2004). This minimum age is consistent with cosmogenic exposure ages of the depositional surface of the El Diablo Formation, which cluster around 12 Ma (data initially presented in Evenstar et al., 2009; recalculated in Evenstar et al., 2015). Since sediments of the Upper Member of the El Diablo Formation were sourced to the east of the Oxaya anticline (e.g., Wörner et al., 2000), this led García and Hérail (2005) to suggest that the topographic barrier created by the anticlinal hinge cannot have existed prior to 12 Ma.

However, there are several reasons why folding could have commenced prior to ca. 12 Ma. First, our reconstruction demonstrates that immediately after eruption, the ignimbrites had a west-dipping, 1.5° ± 0.3° surface that was subsequently deformed by folding. The topographic barrier defined by the hinge zone of the anticline could not have formed immediately, as it would have taken some time for the eastern limb of the fold to rotate from a westward to an eastward dip and form the Copaquilla and Huaylas Basins. We can thus conclude that folding could have started prior to 12 Ma. Furthermore, during this initial deformation phase, fluvial incision into the anticline could have kept pace with its structural growth, forming a series of channels linking the Precordillera/Western Cordillera to the Central Depression. Previous studies (e.g., Wörner et al., 2000, 2002; García and Hérail, 2005) suggested that the Azapa and Lluta Quebradas cut through the upper surface of the El Diablo Formation and thus that river incision commenced after ca. 12 Ma. However, this observation only demonstrates that incision continued after deposition of the El Diablo Formation in the Central Depression, and it does not preclude earlier incision into the Precordillera. We suggest that it is likely that during initial formation of the anticlines, river incision was able to keep pace with uplift, transporting El Diablo Formation sediments westward to the Central Depression. Deposition of these sediments was confined to the western margin of the anticlines, where accommodation space was available (Fig. 9). After 12 Ma, continued

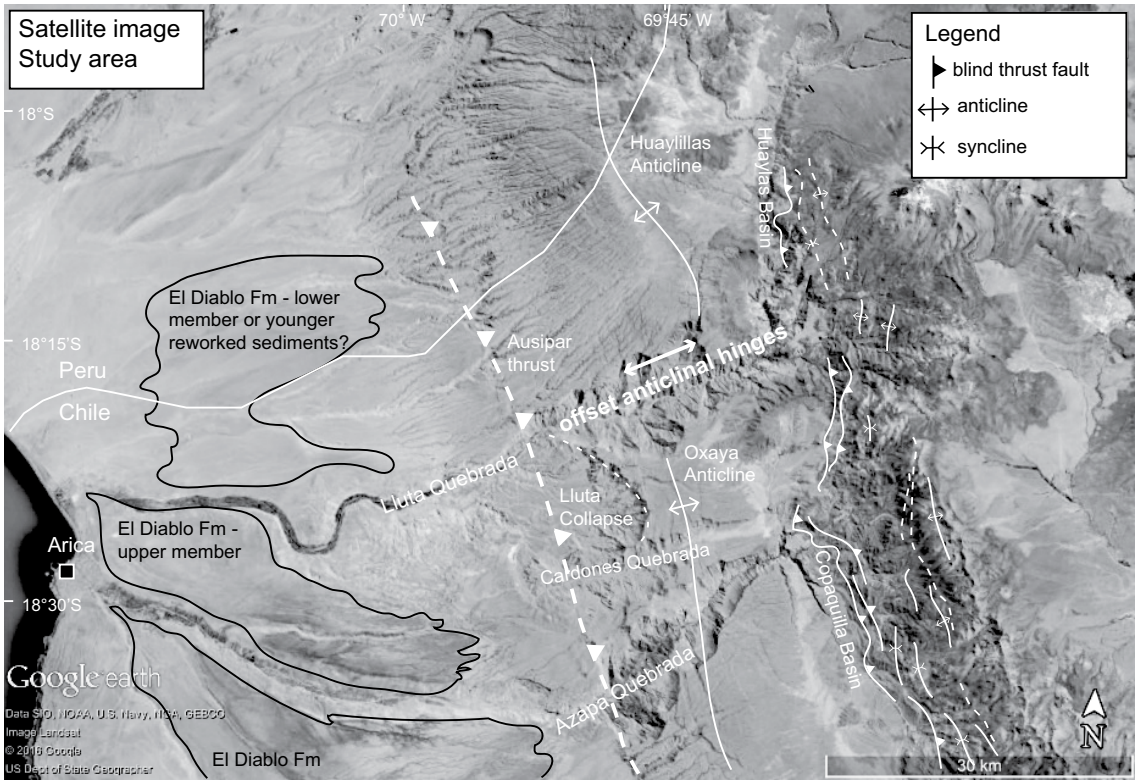

Figure 9. Google Earth Pro satellite image of the study area, with the outlined location of the El Diablo Formation. Note the difference in appearance of the El Diablo Formation from pale north of the Lluta Quebrada to dark south of the Lluta Quebrada.

growth of the anticlines created a topographic barrier that confined sediments to the basins on the eastern margin of the anticlines.

Landscape evolution of the region is inferred to be markedly different north and south of the Lluta Quebrada. In particular, the anticlinal fold hinges of the Oxaya and Huaylillas anticlines appear to be dextrally displaced by >10 km across the Lluta Quebrada (Fig. 9). Furthermore, the appearance of the El Diablo Formation north and south of the Lluta Quebrada is markedly different. We suggest that the intensity and possibly the timing of deformation of the Oxaya and Huaylillas anticlines are different. Our calculated maximum values for fold amplitude (2140 m) and horizontal E-W shortening (~210 m) for the Huaylillas anticline are almost three times as large as those calculated for the Oxaya anticline (fold amplitude 665–840 m; horizontal shortening 60–80 m) by García and Hérail (2005). These authors used the present-day erosional surface as a paleosurface in their reconstructions and did not consider erosion at the hinge of the anticline. Their calculated fold amplitude is therefore likely underestimated. Stratigraphy of the Oxaya ignimbrites shows that the nonwelded upper part of the Oxaya ignimbrite has been eroded from the hinge of the Oxaya anticline. However, even if we account for erosion (maximum of a few hundred meters), the fold amplitude of the Oxaya anticline remains much less than the Huaylillas anticline. Consequently, we conclude that the amplitude of folding decreases from the Huaylillas in the north to the Oxaya anticline and Sucuna monocline (Fig. 1B) in the south.

A marked change across the Lluta valley is indicated by differences in the characteristics of surfaces in the region to the west of the anticlines (Fig. 9). The Upper Member of the El Diablo Formation, with its characteristic dark surface, is absent to the west of the Huaylillas anticline. Here, the surface is pale, and thin deposits (maximum of a few tens of meters) are mostly reworked products of the Oxaya Formation. One interpretation is that these deposits represent the Lower Member of the El Diablo Formation. In this case, the depositional age of this Lower Member is constrained by the Oxaya ignimbrite (19.7 Ma) and the minimum age of the Upper Member of the El Diablo Formation (ca. 12 Ma). However, reworking of the ignimbrite could have continued to more recent times, and thus the ages of this surface and its deposits are not well constrained. We identify three explanations for the absence of the Upper Member of the El Diablo Formation west of the Huaylillas anticline. One explanation is that folding of the Huaylillas anticline initiated earlier than the Oxaya anticline, trapping Upper Member El Diablo sediments in the Huaylas Basin to the east. A second explanation is that the source rocks to the east are different north and south of the Lluta Quebrada. However, we note that mid-Miocene andesitic source rocks of the Upper Member of El Diablo Formation are present throughout the area (purple outcrops in Fig. 1B). Finally, a third explanation is that upper El Diablo sediments could have been transported directly to the Pacific through a gap in the Coastal Cordillera. If this is the case, it raises the question why the Lower Member of the El Diablo Formation was not also transported into the Pacific. One possibility is the entire El Diablo Formation is missing north of the Lluta Quebrada, and all sediments there were later reworked Oxaya Formation sediments.

Finally, we address the offset in the hinge lines of the Huaylillas and Oxaya anticlines. An E-W–trending fault along the Lluta Quebrada can be firmly ruled out by the absence of any lateral offset of the Ausipar thrust, which is thought to have been active since at least the Eocene (e.g., Muñoz and Charrier, 1996). Instead, we suggest that the Lluta Quebrada already existed before folding initiated and was further incised during fold development. The orientation of the Western Cordillera fold-and-thrust belt (Fig. 9) to the east of the anticlines gradually changes from NNE-SSW to almost N-S between the Azapa and Lluta Quebradas. While this change could account for some curvature of the Oxaya anticline hinge zone, it cannot explain the abrupt displacement of the two hinge zones across the Lluta Quebrada. Instead, we propose that, prior to folding, the deep paleovalley that had already incised the Oxaya Formation caused the units on either side to act as mechanically independent layers that responded to buckling in different ways. Thus, this is a case of the landscape influencing fold development.

From our discussion, we conclude that incision of a proto–Lluta River commenced directly after emplacement of the Oxaya Formation ignimbrites. We suggest that formation of both anticlines likely commenced before 12 Ma, and the Huaylillas anticline experienced significantly more structural relief growth compared to the Oxaya anticline. Based on our ca. 6 Ma age for the undeformed, flat-lying lacustrine deposits in the Huaylas Basin to the east of the Huaylillas anticline, we conclude that the main phase of folding of the Huaylillas anticline had ceased by the end of the Miocene (Fig. 8C).

Regional Implications

Compressional foreland fold geometries like the Huaylillas and Oxaya anticlines are typically associated with activation of basement faults (e.g., Narr and Suppe, 1994), such as the Ausipar thrust (García and Hérail, 2001). Our results show that between 90% and 100% of the structural relief growth in the Precordillera can be attributed to basement-involved fault-propagation folding in response to crustal shortening. Similarly, to the south (~19°S–20°S), structural relief growth of the Precordillera is also characterized by west-vergent thrusts that propagate into monoclines and flexures (e.g., Victor et al., 2004; Pinto et al., 2004; Farías et al., 2005). These flexures are thought to have accommodated ~2000 m of relative surface uplift between 19°20′S and 19°50′S (Farías et al., 2005) and ~2600 m of surface uplift around 20°S (Victor et al., 2004). These results are in good agreement with our estimate of up to 2140 m (assuming no erosion) of structural relief growth at the hinge of the Huaylillas anticline (Table 2).

The growth of flexures and monoclines around 19°S–20°S was associated with syndeformation sedimentation. Analyses of growth strata indicate that activity on the faults started as early as 30–26 Ma and lasted until at least 8–7 Ma (Victor et al., 2004; Farías et al., 2005). The onset of deformation in the Oligocene is in good agreement with our reconstructed paleotopography in northernmost Chile, which indicates that development of the Western Andean Slope commenced before 23 Ma.

Our estimate of tilting-related uplift between the eastern edge of the Central Depression and the easternmost edge of the Precordillera is 225 ± 255 m (Table 3; Fig. 6B), which includes the possibility of no tilting. Farías et al. (2005) estimated that, after 10 Ma, the forearc was tilted westward, resulting in additional surface uplift of 500–1400 m over a distance of ~60 km from the eastern edge of the Central Depression across the Precordillera into the Western Cordillera. Adjusting their estimate to a distance of ~50 km gives a range of 400–1200 m, which is still significantly higher than our estimate. We suggest that Farías et al. (2005) overestimated the amount of uplift related to tilting because they used a paleoelevation of 1000 ± 200 m (Charrier et al., 1994) for the Western Cordillera in the late Oligocene–early Miocene. However, our data indicate that the paleoelevation of the eastern edge of the Precordillera might have been up to ~1800 m (Table 3). Consequently, we suggest that tilting played a very minor role, and possibly no role, in Neogene uplift of the Western Andean Slope.

Our results indicate that development of the Western Andean Slope in northernmost Chile spanned at least parts of both the Oligocene and Miocene. This is compatible with other studies in northern Chile (18°S–21°S) that have documented uplift and structural relief growth of the

Western Andean Slope from the early Oligocene (ca. 30 Ma) to the late Miocene (a. 6 Ma), after which structural relief generation diminished (Pinto et al., 2004; Victor et al., 2004; Farías et al., 2005; García and Hérail, 2005; Jordan et al., 2010). Our findings are also consistent with geochemical variations in volcanic rocks around the Central Andean orocline (13°S –18°S) that indicate continuous crustal thickening over the past 30 m.y. (Mamani et al., 2010). In addition, Decou et al. (2013) suggested that sedimentation in the Peruvian forearc (15°S–18°S) occurred between ca. 50 Ma and ca. 4 Ma, implying that uplift of the Western Andean Slope may have started as early as the late Eocene. In general, our study is consistent with slow and steady models for Central Andean uplift over the past ~40 m.y. (e.g., Cooper et al., 2016; Evenstar et al., 2015; Barnes and Ehlers, 2009; Lamb and Davis, 2003).

Overall, studies have shown that Eocene–Oligocene deformation and uplift of the Western Andean Slope and the Altiplano were mainly accommodated by crustal shortening, while addition of significant volumes of magma to the crust and perhaps detachment of the lower crust may also have played important roles during the Miocene (e.g., Isacks, 1988; Lamb and Hoke, 1997; Victor et al., 2004; McQuarrie et al., 2005; Hoke and Lamb, 2007). Evidence for large volumes of magma in the crust includes the Miocene ignimbrite volcanism studied here, as well as mafic backarc volcanism in the Altiplano, both of which were contemporaneous with development of the Western Andean Slope (e.g., de Silva, 1989; Wörner et al., 2000; Victor et al., 2004; Hoke and Lamb, 2007; Kay and Coira, 2009; Freymuth et al., 2015). One possibility is that the associated crustal magmatism heated and weakened the crust along the volcanic front, making it a focal point for deformation (e.g., Isacks, 1988; Allmendinger et al., 1997; Lamb and Hoke, 1997; Hoke and Lamb, 2007; Kay and Coira, 2009). Crustal heating by igneous intrusions below the Altiplano may have resulted in a ductile zone that pinched out beneath the forearc and could have contributed to uplift of the Altiplano.

Several studies (e.g., Isacks, 1988; Lamb et al., 1997) have presented tectonic models that invoke tilting of the forearc. However, we find that regional tilting of the forearc played only a minor or no role in our study area. Thus, inferences of little or no surface tilting across the Precordillera suggest that each of the morphotectonic units acted as fault-bounded blocks, with uplift resulting from shortening combined with largely vertical movements along the thrust faults that bounded the units. In our study area, the Precordillera is bounded by the Ausipar thrust to the west, with a vertical displacement of 200 m, and thrust faults of the Western Cordillera to the east.

CONCLUSIONS

In this study, we used the surface of the deformed early Miocene Cardones ignimbrite in northern Chile to reconstruct the pre-eruption paleotopography and quantify posteruption relief growth on the Western Andean Slope. We demonstrate that outflow sheets of large-volume ignimbrites are able to entirely infill and bury the topography of an area, forming planar surfaces with slopes of less than 2°. If well preserved, such ignimbrites are excellent spatial and temporal markers that can record postemplacement deformation.

Our results suggest that development of the Western Andean Slope in northernmost Chile (~18°20′S) began as early as Oligocene time, most likely in response to crustal shortening and magmatic addition. By ca. 23 Ma, the paleo–Western Andean Slope was up to 960 ± 225 m higher than in the Central Depression, dipped up to 3.7° ± 0.3° westward, and was deeply incised by rivers. This dissected landscape was subsequently infilled and submerged by a series of large-volume ignimbrites in the early Miocene. During deposition, the thickest sequences of ignimbrite accumulated in the deep river valleys. Subsequently, these thick ignimbrites became the most strongly welded and compacted, creating a topographic depression that focused subsequent river incision into similar locations as the pre-ignimbrite paleovalleys. After deposition of the Oxaya Formation, the Western Andean Slope experienced a maximum 1725 ± 165 m of structural relief growth, largely, if not entirely, related to folding in response to contractional deformation. Based on new U-Pb age constraints on volcanic horizons in flat-lying lake sediments, we determined that this folding must have ceased by ca. 6 Ma. Andean uplift as a result of regional tilting, however, was significantly less than previously estimated (e.g., Lamb et al., 1997; Farías et al., 2005) and could have been zero.

ACKNOWLEDGMENTS

This project was funded by BHP Billiton. We would like to thank all people at BHP Billiton, especially Christopher Ford, who provided support in the field and core shed. Funding for U-Pb zircon analyses was provided by Natural Environment Research Council Isotope Geosciences Facilities Steering Committee grant IP-1466-1114 to Cooper. Analytical work would not have been possible without technical support from Nick Roberts, Vanessa Pashley, Simon Tapster, and Nicola Atkinson. The manuscript has benefited from constructive reviews by G. Wörner, S. Kay, C. Garzione, and two unknown reviewers.

REFERENCES CITED

Aldiss, D., and Ghazali, S., 1984, The regional geology and evolution of the Toba volcano-tectonic depression, Indonesia: Journal of the Geological Society, London, v. 141, no. 3, p. 487–500, doi:10.1144/gsjgs.141.3.0487.

Allmendinger, R.W., Jordan, T.E., Kay, S.M., and Isacks, B.L., 1997, The evolution of the Altiplano-Puna Plateau of the Central Andes: Annual Review of Earth and Planetary Sciences, v. 25, no. 1, p. 139–174, doi:10.1146/annurev.earth.25.1.139.

Barnes, J., and Ehlers, T., 2009, End member models for Andean Plateau uplift: Earth-Science Reviews, v. 97, no. 1, p. 105–132, doi:10.1016/j.earscirev.2009.08.003.

Best, M.G., Barr, D.L., Christiansen, E.H., Gromme, S., Deino, A.L., and Tingey, D.G., 2009, The Great Basin Altiplano during the middle Cenozoic ignimbrite flareup: Insights from volcanic rocks: International Geology Review, v. 51, no. 7–8, p. 589–633, doi:10.1080/00206810902867690.

Black, L., and Gulson, B., 1978, The age of the mud tank carbonatite, Strangways Range, Northern Territory: BMR Journal of Australian Geology and Geophysics, v. 3, no. 3, p. 227–232.

Bond, A., and Sparks, R., 1976, The Minoan eruption of Santorini, Greece: Journal of the Geological Society, London, v. 132, no. 1, p. 1–16, doi:10.1144/gsjgs.132.1.0001.

Bowring, S., Schoene, B., Crowley, J., Ramezani, J., and Condon, D., 2006, High-precision U-Pb zircon geochronology and the stratigraphic record: Progress and promise: Paleontological Society Papers, v. 12, p. 25.

Carrasco-Núñez, G., and Branney, M.J., 2005, Progressive assembly of a massive layer of ignimbrite with a normal-to-reverse compositional zoning: The Zaragoza ignimbrite of central Mexico: Bulletin of Volcanology, v. 68, no. 1, p. 3–20, doi:10.1007/s00445-005-0416-8.

Cas, R.A., Wright, H.M., Folkes, C.B., Lesti, C., Porreca, M., Giordano, G., and Viramonte, J.G., 2011, The flow dynamics of an extremely large volume pyroclastic flow, the 2.08-Ma Cerro Galán ignimbrite, NW Argentina, and comparison with other flow types: Bulletin of Volcanology, v. 73, no. 10, p. 1583–1609, doi:10.1007/s00445-011-0564-y.

Charrier, R., Muñoz, N., and Palma-Heldt, S., 1994, Edad y contenido paleoflorístico de la Formación Chucal y condiciones paleoclimáticas para el Oligoceno Tardío-Mioceno Inferior en el Altiplano de Arica, Chile, *in* Proceedings Congreso Geológico Chileno: Actas, v. 1, no. 7, Concepción, p. 434–437.

Charrier, R., Hérail, G., Pinto, L., García, M., Riquelme, R., Farías, M., and Muñoz, N., 2013, Cenozoic tectonic evolution in the Central Andes in northern Chile and west central Bolivia: Implications for paleogeographic, magmatic and mountain building evolution: International Journal of Earth Sciences, v. 102, no. 1, p. 235–264, doi:10.1007/s00531-012-0801-4.

Coira, B., Davidson, J., Mpodozis, C., and Ramos, V., 1982, Tectonic and magmatic evolution of the Andes of northern Argentina and Chile: Earth-Science Reviews, v. 18, no. 3, p. 303–332, doi:10.1016/0012-8252(82)90042-3.

Cooper, F.J., Adams, B.A., Blundy, J.D., Farley, K.A., McKeon, R.E., and Ruggiero, A.A., 2016, Aridity-induced Miocene canyon incision in the Central Andes: Geology, v. 44, p. 675–678, doi:10.1130/G38254.1.

Decou, A., Von Eynatten, H., Dunkl, I., Frei, D., and Wörner, G., 2013, Late Eocene to early Miocene Andean uplift inferred from detrital zircon fission track and U-Pb dating of Cenozoic forearc sediments (15–18°S): Journal of South American Earth Sciences, v. 45, p. 6–23, doi:10.1016/j.jsames.2013.02.003.

de Silva, S., 1989, Altiplano-Puna volcanic complex of the Central Andes: Geology, v. 17, no. 12, p. 1102–1106, doi:10.1130/0091-7613(1989)017<1102:APVCOT>2.3.CO;2.

Dunai, T.J., López, G.A.G., and Juez-Larré, J., 2005, Oligocene–Miocene age of aridity in the Atacama Desert revealed by exposure dating of erosion-sensitive landforms: Geology, v. 33, no. 4, p. 321–324, doi:10.1130/G21184.1.

Evenstar, L.A., Hartley, A.J., Stuart, F.M., Mather, A.E., Rice, C.M., and Chong, G., 2009, Multiphase development of the Atacama planation surface recorded by cosmogenic ^{3}He exposure ages: Implications for uplift and Cenozoic climate change in western South America: Geology, v. 37, no. 1, p. 27–30, doi:10.1130/G25437A.1.

Evenstar, L.A., Stuart, F.M., Hartley, A.J., and Tattitch, B., 2015, Slow Cenozoic uplift of the western Andean Cordillera indicated by cosmogenic ^{3}He in alluvial boulders from the Pacific planation surface: Geophysical Research Letters, v. 42, no. 20, p. 8448–8455, doi:10.1002/2015GL065959.

Farías, M., Charrier, R., Comte, D., Martinod, J., and Hérail, G., 2005, Late Cenozoic deformation and uplift of the western flank of the Altiplano: Evidence from the depositional, tectonic, and geomorphological evolution and shallow seismic activity (northern Chile at 19°30′S): Tectonics, v. 24, no. 4, doi:10.1029/2004TC001667.

Freymuth, H., Brandmeier, M., and Wörner, G., 2015, The origin and crust/mantle mass balance of Central Andean ignimbrite magmatism constrained by oxygen and strontium isotopes and erupted volumes: Contributions to Mineralogy and Petrology, v. 169, no. 6, p. 1–24, doi:10.1007/s00410-015-1152-5.

García, M., and Hérail, G., 2001, Comment on: 'Geochronology (Ar-Ar, K-Ar and He-exposure ages) of Cenozoic magmatic rocks from northern Chile (18–22°S): Implications for magmatism and tectonic evolution of the Central Andes' of Wörner et al. (2000): Revista Geológica de Chile, v. 28, no. 1, p. 127–130.

García, M., and Hérail, G., 2005, Fault-related folding, drainage network evolution and valley incision during the Neogene in the Andean Precordillera of northern Chile: Geomorphology, v. 65, no. 3, p. 279–300, doi:10.1016/j.geomorph.2004.09.007.

García, M., Gardeweg, M., Hérail, G., and Pérez de Arce, C., 2000, La Ignimbrita Oxaya y la Caldera Lauca: Un evento explosive de gran volumen del Mioceno Inferior en la región de Arica (Andes Centrales 18–19°S), *in* IX Congreso Geologico Chileno, Actas Volume 2: Puerto Varas, Chile, p. 286–290.

García, M., Gardeweg, M., Clavero, J., and Hérail, G., 2004, Arica Map: Tarapacá Region, scale 1:250,000: Santiago, Servicio Nacional de Geología y Minería, Carta Geológica de Chile Serie Geología básica, v. 84.

García, M., Riquelme, R., Farías, M., Hérail, G., and Charrier, R., 2011, Late Miocene–Holocene canyon incision in the western Altiplano, northern Chile: Tectonic or climatic forcing?: Journal of the Geological Society, London, v. 168, no. 4, p. 1047–1060, doi:10.1144/0016-76492010-134.

Gaupp, R., Kött, A., and Wörner, G., 1999, Palaeoclimatic implications of Mio–Pliocene sedimentation in the high-altitude intra-arc Lauca Basin of northern Chile: Palaeogeography, Palaeoclimatology, Palaeoecology, v. 151, no. 1, p. 79–100, doi:10.1016/S0031-0182(99)00017-6.

Hayashi, J., and Self, S., 1992, A comparison of pyroclastic flow and debris avalanche mobility: Journal of Geophysical Research–Solid Earth (1978–2012), v. 97, no. B6, p. 9063–9071.

Henry, C.D., and Faulds, J.E., 2010, Ash-flow tuffs in the Nine Hill, Nevada, paleovalley and implications for tectonism and volcanism of the western Great Basin, USA: Geosphere, v. 6, no. 4, p. 339–369, doi:10.1130/GES00548.1.

Hoke, L., and Lamb, S., 2007, Cenozoic behind-arc volcanism in the Bolivian Andes, South America: Implications for mantle melt generation and lithospheric structure: Journal of the Geological Society, London, v. 164, no. 4, p. 795–814, doi:10.1144/0016-76492006-092.

Isacks, B. L., 1988, Uplift of the central Andean plateau and bending of the Bolivian orocline: Journal of Geophysical Research–Solid Earth (1978–2012), v. 93, no. B4, p. 3211–3231.

Jordán, T.E., Isacks, B.L., Allmendinger, R.W., Brewer, J.A., Ramos, V.A., and Ando, C.J., 1983, Andean tectonics related to geometry of subducted Nazca plate: Geological Society of America Bulletin, v. 94, no. 3, p. 341–361, doi:10.1130/0016-7606(1983)94<341:ATRTGO>2.0.CO;2.

Jordan, T.E., Nester, P., Blanco, N., Hoke, G., Davila, F., and Tomlinson, A., 2010, Uplift of the Altiplano-Puna Plateau: A view from the west: Tectonics, v. 29, TC5007, no. 5, doi:10.1029/2010TC002661.

Kay, S.M., and Coira, B.L., 2009, Shallowing and steepening subduction zones, continental lithospheric loss, magmatism, and crustal flow under the Central Andean Altiplano-Puna Plateau, *in* Kay, S.M., Ramos, V.A., and Dickinson, W.R., eds., Backbone of the Americas: Shallow Subduction, Plateau Uplift, and Ridge and Terrane Collision: Geological Society of America Memoir 204, p. 229–259.

Kober, F., Ivy-Ochs, S., Schlunegger, F., Baur, H., Kubik, P., and Wieler, R., 2007, Denudation rates and a topography-driven rainfall threshold in northern Chile: Multiple cosmogenic nuclide data and sediment yield budgets: Geomorphology, v. 83, no. 1, p. 97–120, doi:10.1016/j.geomorph.2006.06.029.

Kött, A., Gaupp, R., and Wörner, G., 1995, Miocene to Recent history of the western Altiplano in northern Chile revealed by lacustrine sediments of the Lauca Basin (18°15′–18°40′S/69°30′–69°05′W): Geologische Rundschau, v. 84, no. 4, p. 770–780, doi:10.1007/s005310050039.

Lamb, S., and Davis, P., 2003, Cenozoic climate change as a possible cause for the rise of the Andes: Nature, v. 425, no. 6960, p. 792–797, doi:10.1038/nature02049.

Lamb, S., and Hoke, L., 1997, Origin of the high plateau in the Central Andes, Bolivia, South America: Tectonics, v. 16, no. 4, p. 623–649, doi:10.1029/97TC00495.

Lamb, S., Hoke, L., Kennan, L., and Dewey, J., 1997, Cenozoic evolution of the Central Andes in Bolivia and northern Chile, *in* Burg, J.-P., and Ford, M., eds., Orogeny through Time: Geological Society, London, Special Publication 121, p. 237–264, doi:10.1144/GSL.SP.1997.121.01.10.

Lanphere, M.A., Champion, D.E., Christiansen, R.L., Izett, G.A., and Obradovich, J.D., 2002, Revised ages for tuffs of the Yellowstone Plateau volcanic field: Assignment of the Huckleberry Ridge Tuff to a new geomagnetic polarity event: Geological Society of America Bulletin, v. 114, no. 5, p. 559–568, doi:10.1130/0016-7606(2002)114<0559:RAFTOT>2.0.CO;2.

Ludwig, K.R., 2003, User's Manual for Isoplot 3.00: A Geochronological Toolkit for Microsoft Excel: Berkeley Geochronology Center Special Publication 4, 73 p.

Mamani, M., Wörner, G., and Sempere, T., 2010, Geochemical variations in igneous rocks of the Central Andean orocline (13°S to 18°S): Tracing crustal thickening and magma generation through time and space: Geological Society of America Bulletin, v. 122, no. 1–2, p. 162–182, doi:10.1130/B26538.1.

Martinod, J., Husson, L., Roperch, P., Guillaume, B., and Espurt, N., 2010, Horizontal subduction zones, convergence velocity and the building of the Andes: Earth and Planetary Science Letters, v. 299, no. 3, p. 299–309, doi:10.1016/j.epsl.2010.09.010.

McQuarrie, N., Horton, B.K., Zandt, G., Beck, S., and DeCelles, P.G., 2005, Lithospheric evolution of the Andean fold–thrust belt, Bolivia, and the origin of the central Andean plateau: Tectonophysics, v. 399, no. 1, p. 15–37, doi:10.1016/j.tecto.2004.12.013.

Montgomery, D.R., and Brandon, M.T., 2002, Topographic controls on erosion rates in tectonically active mountain ranges: Earth and Planetary Science Letters, v. 201, no. 3, p. 481–489, doi:10.1016/S0012-821X(02)00725-2.

Muñoz, N., and Charrier, R., 1996, Uplift of the western border of the Altiplano on a west-vergent thrust system, northern Chile: Journal of South American Earth Sciences, v. 9, no. 3, p. 171–181, doi:10.1016/0895-9811(96)00004-1.

Myers, J., 1976, Erosion surfaces and ignimbrite eruption, measures of Andean uplift in northern Peru: Geological Journal, v. 11, no. 1, p. 29–44, doi:10.1002/gj.3350110104.

Narr, W., and Suppe, J., 1994, Kinematics of basement-involved compressive structures: American Journal of Science, v. 294, no. 7, p. 802–860, doi:10.2475/ajs.294.7.802.

Pinto, L., Hérail, G., and Charrier, R., 2004, Sedimentación sintectónica asociada a las estructuras neógenas en la Precordillera de la zona de Moquella, Tarapacá (19°15′S, norte de Chile): Revista Geológica de Chile, v. 31, no. 1, p. 19–44.

Ponomareva, V., Kyle, P., Melekestsev, I., Rinkleff, P., Dirksen, O., Sulerzhitsky, L., Zaretskaia, N., and Rourke, R., 2004, The 7600 (14C) year BP Kurile Lake caldera-forming eruption, Kamchatka, Russia: Stratigraphy and field relationships: Journal of Volcanology and Geothermal Research, v. 136, no. 3, p. 199–222, doi:10.1016/j.jvolgeores.2004.05.013.

Roche, O., Buesch, D.C., and Valentine, G.A., 2016, Slow-moving and far-travelled dense pyroclastic flows during the Peach Spring super-eruption: Nature Communications, v. 7, p. 10890, doi:10.1038/ncomms10890.

Salas, R., Kast, R., and Montecinos, F., Salas 1., 1966, Geología y Recursos Minerales del Departamento de Arica, Provincia de Tarapacá: Instituto de Investigaciones Geológicas Boletín 21, 114 p.

Schoene, B., Crowley, J.L., Condon, D.J., Schmitz, M.D., and Bowring, S.A., 2006, Reassessing the uranium decay constants for geochronology using ID-TIMS U-Pb data: Geochimica et Cosmochimica Acta, v. 70, no. 2, p. 426–445, doi:10.1016/j.gca.2005.09.007.

Smith, R.L., and Bailey, R.A., 1966, The Bandelier Tuff: A study of ash-flow eruption cycles from zoned magma chambers: Bulletin of Volcanology, v. 29, no. 1, p. 83–103, doi:10.1007/BF02597146.

Somoza, R., 1998, Updated Nazca (Farallon)–South America relative motions during the last 40 My: Implications for mountain building in the central Andean region: Journal of South American Earth Sciences, v. 11, no. 3, p. 211–215, doi:10.1016/S0895-9811(98)00012-1.

Sparks, R.S.J., 1975, The stratigraphy and geology of the ignimbrites of Vulsini volcano, central Italy: Geologische Rundschau, v. 64, no. 1, p. 497–523, doi:10.1007/BF01820680.

Sparks, R.S.J., 1976, Grain size variations in ignimbrites and implications for the transport of pyroclastic flows: Sedimentology, v. 23, no. 2, p. 147–188, doi:10.1111/j.1365-3091.1976.tb00045.x.

van Zalinge, M., Sparks, R., Cooper, F., and Condon, D., 2016, Early Miocene large-volume ignimbrites of the Oxaya Formation, Central Andes: Journal of the Geological Society, London, v. 173, p. 716–733, doi:10.1144/jgs2015-123.

Victor, P., Oncken, O., and Glodny, J., 2004, Uplift of the western Altiplano plateau: Evidence from the Precordillera between 20 and 21°S (northern Chile): Tectonics, v. 23, no. 4, TC4004, doi:10.1029/2003TC001519.

Walker, G.P.L., 1983, Ignimbrite types and ignimbrite problems: Journal of Volcanology and Geothermal Research, v. 17, no. 1, p. 65–88, doi:10.1016/0377-0273(83)90062-8.

Walker, G.P.L., Heming, R., and Wilson, C., 1980, Low-aspect ratio ignimbrites: Nature, v. 283, p. 286–287.

Wendt, I., and Carl, C., 1991, The statistical distribution of the mean squared weighted deviation: Chemical Geology–Isotope Geoscience Section, v. 86, no. 4, p. 275–285, doi:10.1016/0168-9622(91)90010-T.

Wilson, C., 1991, Ignimbrite morphology and the effects of erosion: A New Zealand case study: Bulletin of Volcanology, v. 53, no. 8, p. 635–644, doi:10.1007/BF00493690.

Wilson, C.J., and Hildreth, W., 1997, The Bishop Tuff: New insights from eruptive stratigraphy: The Journal of Geology, v. 105, no. 4, p. 407–440, doi:10.1086/515937.

Wörner, G., Hammerschmidt, K., Henjes-Kunst, F., Lezaun, J., and Wilke, H., 2000, Geochronology ($^{40}Ar/^{39}Ar$, K-Ar and He-exposure ages) of Cenozoic magmatic rocks from northern Chile (18–22°S): Implications for magmatism and tectonic evolution of the central Andes: Revista Geológica de Chile, v. 27, no. 2, p. 205–240.

Wörner, G., Uhlig, D., Kohler, I., and Seyfried, H., 2002, Evolution of the West Andean Escarpment at 18°S (N. Chile) during the last 25 Ma: Uplift, erosion and collapse through time: Tectonophysics, v. 345, no. 1, p. 183–198, doi:10.1016/S0040-1951(01)00212-8.

Wotzlaw, J.F., Decou, A., von Eynatten, H., Wörner, G., and Frei, D., 2011, Jurassic to Palaeogene tectono-magmatic evolution of northern Chile and adjacent Bolivia from detrital zircon U-Pb geochronology and heavy mineral provenance: Terra Nova, v. 23, no. 6, p. 399–406.

Wright, J.V., Smith, A.L., and Self, S., 1980, A working terminology of pyroclastic deposits: Journal of Volcanology and Geothermal Research, v. 8, no. 2, p. 315–336, doi:10.1016/0377-0273(80)90111-0.

Yokoyama, S., 1974, Mode of movement and emplacement of Ito pyroclastic flow from Aira caldera, Japan: Tokyo Kyoiku Daigaku Scientific Reports, v. 12, p. 17–62.

MANUSCRIPT RECEIVED 18 JULY 2016
REVISED MANUSCRIPT RECEIVED 3 OCTOBER 2016
MANUSCRIPT ACCEPTED 8 NOVEMBER 2016

Printed in the USA